NANO · MICRO small
www.small-journal.com

# Liquid–Liquid Interfacial Nanoarchitectonics

*Katsuhiko Ariga*

**Science in the small world has become a crucial key that has the potential to revolutionize materials technology. This trend is embodied in the postnanotechnology concept of nanoarchitectonics. The goal of nanoarchitectonics is to create bio-like functional structures, in which self-organized and hierarchical structures are working efficiently. Liquid–liquid interface like environments such as cell membrane surface are indispensable for the expression of biological functions through the accumulation and organization of functional materials. From this viewpoint, it is necessary to reconsider the liquid–liquid interface as a medium where nanoarchitectonics can play an active role. In this review, liquid–liquid interfacial nanoarchitectonics is classified by component materials such as organic, inorganic, carbon, and bio, and recent research examples are discussed. Examples discussed in this paper include molecular aggregates, supramolecular polymers, conductive polymers film, crystal-like capsules, block copolymer assemblies, covalent organic framework (COF) films, complex crystals, inorganic nanosheets, colloidosomes, fullerene assemblies, all-carbon $\pi$-conjugated graphite nanosheets, carbon nanoskins and fullerphene thin films at liquid–liquid interfaces. Furthermore, at the liquid–liquid interface using perfluorocarbons and aqueous phases, cell differentiation controls are discussed with the self-assembled structure of biomaterials. The significance of liquid–liquid interfacial nanoarchitectonics in the future development of materials will then be discussed.**

## 1. Introduction

Humans have developed functional materials and structures necessary for social life by discovering materials, processing them, and creating new materials. In the 20th century, various fields of science have developed to synthesize new materials and clarify the mechanisms by which functions are achieved. The turning point in this development was the initiation of nanotechnology. Direct observation of nanostructures down to the atomic and molecular levels[1–3] has made it possible to understand physical properties in the nanoscale region.[4–6] The mechanisms by which materials produce high functionality and the methodologies to create more advanced functions through nanostructure control were explored. In other words, science in the small world has become a crucial key that has the potential to revolutionize materials science.[7–9] This trend is embodied in the postnanotechnology concept of nanoarchitectonics (**Figure 1**).[10] Nanotechnology was initiated by Richard Feynman in the mid-20th century,[11,12] and nanoarchitectonics was proposed by Masakazu Aono in the early 21st century.[13,14] It is the architecture of functional materials using atoms, molecules, and nanomaterials as the building blocks.[15–17] This concept has been similarly considered as a bottom-up approach in supramolecular chemistry[18–20] and coordination chemistry.[21–23] Nanoarchitectonics encompasses this approach and integrates nanotechnology with various material-related chemistry, microfabrication technology, biotechnology, and so on.[24,25] The nanoarchitectonics approach has an integrative significance for the synthesis of materials from nanotechnology. Since all materials are made of atoms and molecules, nanoarchitectonics can be applied to all functional materials. In analogy to the theory of everything in physics,[26] nanoarchitectonics may be considered a method for everything in materials science.[27]

If we extend the scope of nanoarchitectonics beyond human technology, we can say that living organisms create superior functional systems by assembling molecules as nanounits. It can be, in principle, said that biological systems are formed by nanoarchitectonics.[28–30] However, this is done at a considerable level of sophistication. A large number of components rationally form a hierarchical organization, and their functions work in coordination and harmony with each other. The formation of hierarchical structures[31,32] and the harmonization of various interactions in fluctuations[33] are also characteristics of nanoarchitectonics. The goal of nanoarchitectonics is to create such bio-like functional structures,[34–36] which organisms have already done over time during billions of years of evolution.[37] Self-organized, hierarchical, and three-dimensional structures are

K. Ariga
Research Center for Materials Nanoarchitectonics
National Institute for Materials Science (NIMS)
1-1 Namiki, Tsukuba 305-0044, Japan
E-mail: ARIGA.Katsuhiko@nims.go.jp
K. Ariga
Graduate School of Frontier Sciences
The University of Tokyo
5-1-5 Kashiwa-no-ha Kashiwa, Tokyo 277–8561, Japan

The ORCID identification number(s) for the author(s) of this article can be found under https://doi.org/10.1002/smll.202305636



**DOI: 10.1002/smll.202305636**

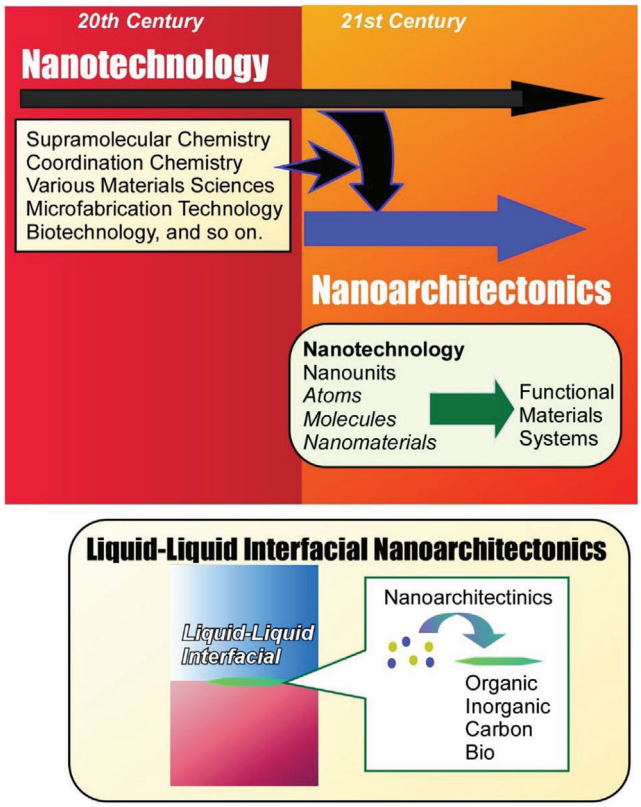


**Figure 1.** Outline of nanoarchitectonics concept and application to liquid–liquid interfacial systems.

being spontaneously nanoarchitectonized. In many cases, two-dimensional systems, such as biomaterials interfaces, are being skillfully used. Although the inner surfaces of protein pockets and polymer interfaces formed with DNA and other molecules are powerful interfaces, the most powerful two-dimensional interface field is the cell membrane.[38,39] Using the spatially restricted environment of the cell membrane surface and the spatial extent of the interior of the cell membrane, organisms skillfully let the functional molecules create hierarchical, highly functional systems. In addition, the intertwining and harmonization of several functions using such membranes as a medium generates excellent functions such as photosynthesis[40,41] and signal transduction.[42,43] The cell membrane is a very fluid environment, which is very advantageous for functional coordination. This environment is more like a liquid–liquid interface than a liquid–solid interface. It is an environment similar to the interface between water and oily fats. In addition, it has been elucidated that liquid-like phase-separation structures and phenomena are very important for biological functions.[44,45] In other words, the liquid–liquid interface is an indispensable place for the expression of biological functions through the accumulation and organization of functional materials. The nanoarchitectonics of biomolecules at the liquid–liquid interface is the key to biological activities.

Let us take a fresh look at the nanoarchitectonics of artificial functional systems. As in biological systems, interfaces, which are two-dimensionally confine media, are a powerful site for the construction of functional systems by nanoarchitectonics. Interfacial nanoarchitectonics also plays an important role in artificial functional systems.[46–48] On-surface synthesis[49,50] and local probe chemistry[51,52] are good examples of nanotechnology and nanoarchitectonics on solid substrates. Molecular nanoarchitectonics[53–55] is being developed at the solid interface, such as synthesizing two-dimensional nanocarbons by linking molecules together or using probe microscope tips to perform addition reactions on specific sites of molecules.[56,57] Layer-by-layer (LbL) assembly is known as a nanoarchitectonics method based on the accumulation of materials from a liquid interface to a solid interface.[58–60] LbL assembly is a methodology that allows the flexible integration of various materials as two-dimensional layered structures. It is also used for nanoarchitectonics of hierarchical structures in combination with self-assembly and template synthesis.[61,62] A classic example of nanoarchitectonics using gas–liquid surfaces is the Langmuir–Blodgett (LB) method.[63–65] This method is a traditional technique with a history of more than 100 years.[66,67] However, in contrast to the conventionally used operation at around room temperature, operations at ultrahigh temperatures approaching 200 °C have recently been reported.[68,69] In addition, the vortex LB method, which uses the dynamic motion of vortex flow in the aqueous phase, has been proposed[70–72] in contrast to the conventional method that requires a clean and undisturbed inner surface. There is ample room for further development of this method.

The LbL assembly for the liquid–solid interface and the LB method for the gas–liquid interface are often discussed in review articles as the well-known methodologies. On the other hand, the liquid–liquid interface, in which both parties are in the liquid phase, has long been considered for material synthesis, such as synthesis using the emulsion interface,[73–75] but has not been actively considered in the critical aspect of nanostructure formation. The interface between liquids with different polarities is a unique meeting place for substances with different solubilities. The combinations of such liquids are innumerable. It is a field where dynamic behavior is allowed with less constraints on motion. It can take on a variety of sizes, from nano- and microscopic sizes, such as nanoemulsions and microemulsions, to liquid interfaces of visible sizes. It is a place where the size and polarity of the environment can be freely designed while being diverse and dynamic. The liquid–liquid interface will become an environment for nanoarchitectonics, where processes can be designed with a free mind. It is necessary to reconsider the liquid–liquid interface as a place where nanoarchitectonics can play an active role. In this review, liquid–liquid interfacial nanoarchitectonics is classified by component materials such as (i) organic, (ii) inorganic, (iii) carbon, and (iv) bio, and recent research examples are discussed. The significance of liquid–liquid interfacial nanoarchitectonics in the development of materials will then be discussed.

## 2. Liquid–Liquid Interfacial Nanoarchitectonics, Organic

At the liquid–liquid interface, a wide variety of nanostructures are formed by the assembly and reaction of molecules and substances. The variety of structures is especially remarkable in processes using organic molecules, which change shape softly and

have low structural symmetry. First, example of liquid–liquid interfacial nanoarchitectonics for organic molecules is discussed in the following section.

There are various processes of nanostructure formation by supramolecular assemblies. Such processes are not only due to thermodynamic equilibrium, but also to kinetic processes that create structures different from the most stable structures. Scanlon and co-workers have studied assembling behaviors of zinc(II) mesotetrakis(4-carboxyphenyl)porphyrin at the water–organic solvent ($\alpha,\alpha,\alpha$-trifluorotluene) interface, which are analyzed by time-resolved in situ UV–Vis spectroscopy (**Figure 2**A).[76] A metastable J-type nanoaggregate structure with a kinetic advantage was initially formed rapidly. This was followed by the thermodynamically favorable H-type aggregate formation. Such an association pathway can be controlled by external factors. When the electrostatic environment of the interface was tuned by adding a cosmotropic anion (citrate), only J-type aggregates were formed at high concentrations. This is the result of complete forcing of the kinetically favorable interfacial nanostructure formation pathway. Such pathway complexity is also effective in interfacial environments. Thus, optimal nanostructures can be rationally nanoarchitected from the same components by tuning thermodynamics and kinetics at the liquid–liquid interface. Such tactics could also be applied to control the assembly structures of organic molecules other than porphyrins and natural proteins to provide optimal nanostructures for photovoltaic, molecular electronics, and biomedical technologies.

The nanoarchitectonics of conductive polymers into thin films has potential applications in energy conversion, energy storage, sensors, biomedical applications, and so on. Gamero-Quijano, Scanlon, and co-workers have directly fabricated thin films of poly(3,4-ethylenedioxythiophene) (PEDOT) by electrochemical synthesis at the liquid–liquid interface (Figure 2B).[77] The formed structures cannot be obtained in bulk solution or at the solid electrode–electrolyte interface. At the liquid–liquid interface, the nucleation and growth of the PEDOT thin film were electrochemically controlled to create two-dimensional and three-dimensional structures. The two-dimensional structures were flat on both sides and less than 50 nm thick. On the other hand, the three-dimensional structure with Janus structure, which was more than 850 nm thick, had flat and rough surfaces and showed different physical properties. The resulting PEDOT thin films have p-doping properties close to the theoretical limit, exhibit high $\pi$-$\pi$ conjugation, and are highly conductive without post-treatment. The reagents required for this process are minimal and the process is gentle, which is very advantageous for large-scale thin film production. In addition, PEDOT thin films prepared by liquid–liquid interfacial electrolysis showed excellent biocompatibility. The thin films can be used as scaffolds for cell growth without the need for chemical modification. In addition, bioactive molecules can be easily incorporated into the PEDOT polymer and customized for cell growth studies. For example, applications could include organic electrochemical transistor devices that can monitor cell behavior for extended periods of time.

Micelles and vesicles composed of lipids and polymers are useful for drug delivery and gene therapy, but often lack sufficient mechanical strength. Colloidal particles could be used to enhance their structural stability, but the crystallization and curvature of colloidal particles may be incompatible with vesicle-like structure. As an overcoming of these difficulties, Li and co-workers have successfully grown nanosized polymer single-crystal-like capsules using a crystallization method at the liquid–liquid interface of a miniemulsion.[78] The structures are formed of polymer lamellar crystals and are given the name crystasomes. The growth of single crystals of poly(L-lactic acid) was promoted at the curved interface created from water and xylene, resulting in nanoarchitectonics of crystals ranging in size from about 148 nm to over 1 μm. The flexural modulus of crystasomes was confirmed by atomic microscopy techniques to be two to three orders of magnitude higher than that of normal polymersomes. Although conventional polymer vesicles are composed of amphiphilic block copolymers, the crystalsomes are made of crystalline homopolymers. The fundamental difference is that polymers grow at the liquid–liquid interface in the direction of polymer single crystals. In addition to the basic science of crystallization in curved space, this will contribute to application-oriented basic research such as polymer nanoarchitectonics for drug delivery and gene therapy.

Pramanik, Karan, Das, and coworkers synthesized freestanding polyimine nanofilms up to 14 nm thick by self-assembly of imine oligomers at the liquid–liquid interface and investigated ultrathin film nanofiltration applications (**Figure 3**A).[79] Specifically, the nanofilms were oligomerized with tris(4-formyl phenyl)benzene and ethylenediamine in xylene and self-assembled at the water-xylene interface for 3 h to form two-dimensional thin films. The self-assembled nanofilms were transferred to polyacrylonitrile ultrafiltration supports to form composite membranes for nanofiltration applications, allowing complete exclusion of brilliant blue R and separation of small dyes such as methyl orange from a mixed dye feed. It also showed high permeability with high removal ration of monovalent and divalent salts. Ultrathin film nanoarchitectonics through polymerization and self-assembly at the liquid–liquid interface can be used to create ultrathin separation layers of composite membranes. The resulting ultrathin materials are expected to be useful as nanofiltration membranes for many applications, from basic processes such as molecular separation to practical separation in wastewater treatment and the pharmaceutical industry.

Liu and co-workers systematically studied the self-assembly process of block copolymers (polystyrene-block-poly(2-vinylpyridine)) at the liquid–liquid interface (Figure 3B).[80] The block copolymer was dissolved in chloroform solution, and the structures formed at interface with the aqueous phase containing chloroauric acid. Four major morphologies of block copolymers were observed as primary forms of aggregates: nanodot arrays, parallel nanostrands, layered films, and long nanobelts. The formation of these structures depends mainly on the molecular structure of the block copolymers, the interaction between the block copolymers at the interface, and the interaction between the block copolymer and the two-phase. Further analysis of the formation mechanism indicates that these structures are the result of adsorption/self-assembly at the block copolymer interface and nucleation/epitaxial growth of further generated aggregates. As additional structures, large-area organization into honeycomb monolayers and foams was also observed. The latter two structures are based on the water pore template effect at the liquid–liquid interface and interfacial spontaneous emulsification. In particular, the aqueous pore template method at the liquid–liquid interface is expected to be applicable

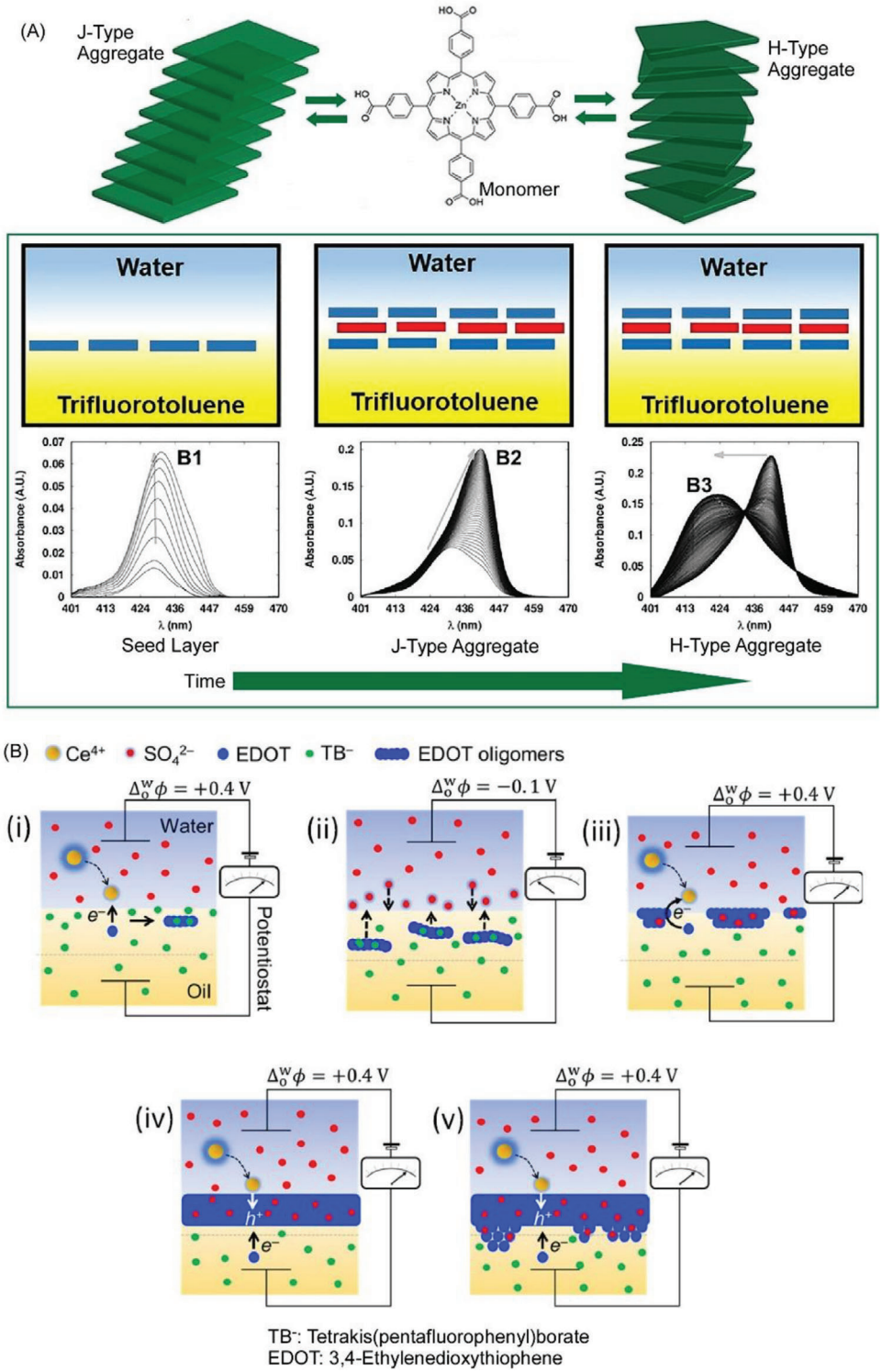


**Figure 2.** A) Assembling behaviors of zinc(II) mesotetrakis(4-carboxyphenyl)porphyrin at the water–organic solvent ($\alpha$,$\alpha$,$\alpha$-trifluorotluene) interface. Reproduced under terms of the CC-BY license.[76] Copyright, 2021, American Chemical Society. B) Fabrication of thin films of poly(3,4-ethylenedioxythiophene) (PEDOT) by electrochemical synthesis at the liquid–liquid interface. Reproduced under terms of the CC-BY license.[77] Copyright 2022, American Chemical Society.

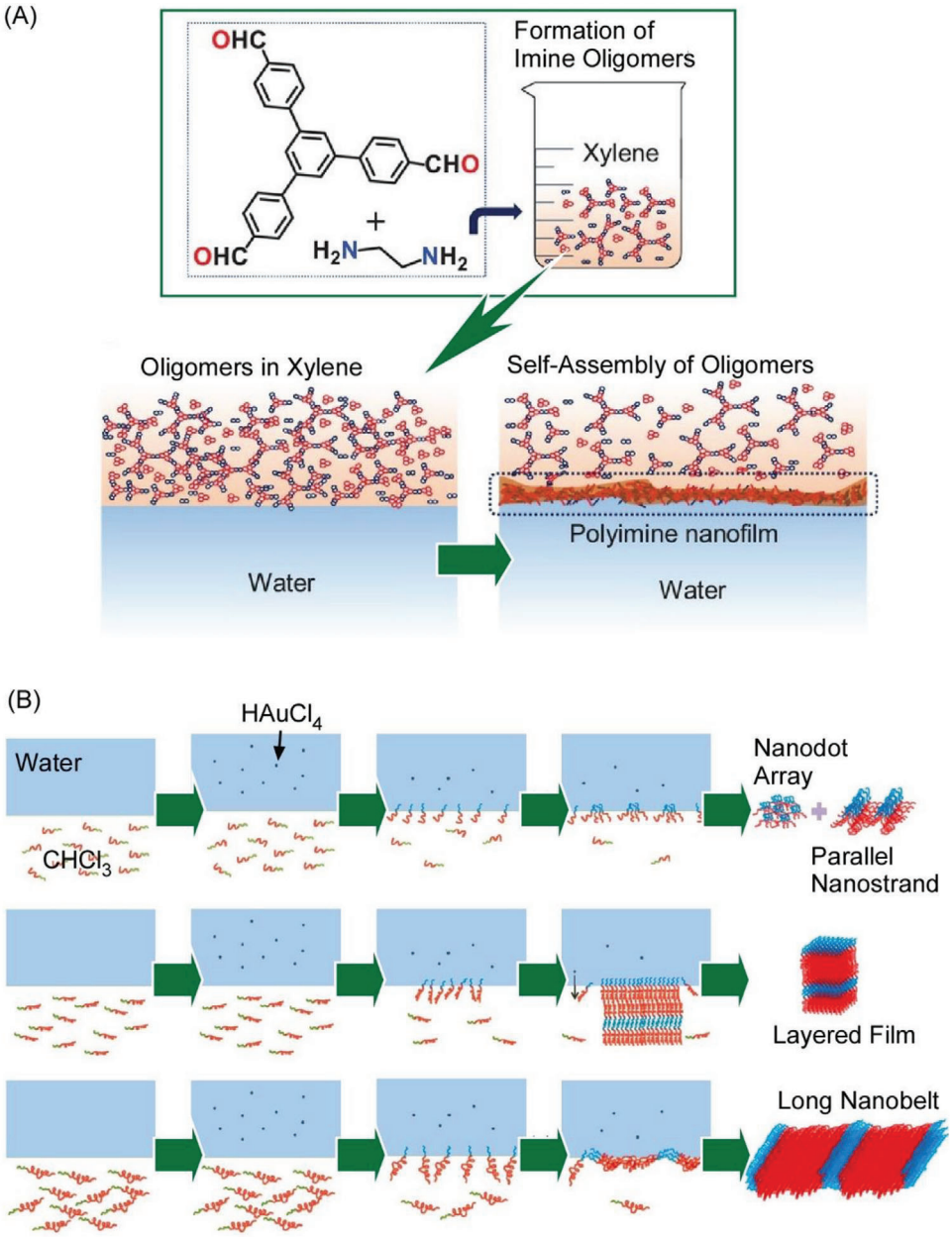


**Figure 3.** A) Synthesis of freestanding polyimine nanofilms by self-assembly of tris(4-formyl phenyl)benzene and ethylenediamine at the water–xylene interface. Reproduced with permission.[79] Copyright 2020, Wiley-VCH. B) Self-assembly process of block copolymers (polystyrene-block-poly(2-vinylpyridine)) at the liquid–liquid interface to provide various nanoarchitectures such as nanodot arrays, parallel nanostrands, layered films, and long nanobelts. Reproduced with permission.[80] Copyright 2022, American Chemical Society.

to the preparation of functional honeycomb monolayers of various materials because of its simplicity and convenience.

Semenov, Giuseppone, and co-workers studied supramolecular polymerization of triarylamine molecules at the chloroform–water interface and their photoinduced organization (**Figure 4**A).[81] Triarylamines in chloroform undergo supramolecular polymerization upon partial photooxidation and are organized into helical fibrils. Gold nanoparticles coated with negatively charged citric acid molecules from the aqueous phase associate with the interfacial nematic layer of the resulting one-dimensional supramolecular polymer fibrils. The supramolecular polymer acts as a template for the precise alignment of the gold nanoparticles coming from the aqueous phase. The strings of polymer chains and nanoparticles obtained by such nanoarchitectonic processes at the liquid–liquid interface can be highly anisotropically co-located over very large distances. Investigation by electron energy loss spectroscopy reveals that the nanoparticles organized in the strings behave as plasmon waveguides. Such an organization will be useful not only for basic studies of plasmon coupling between gold

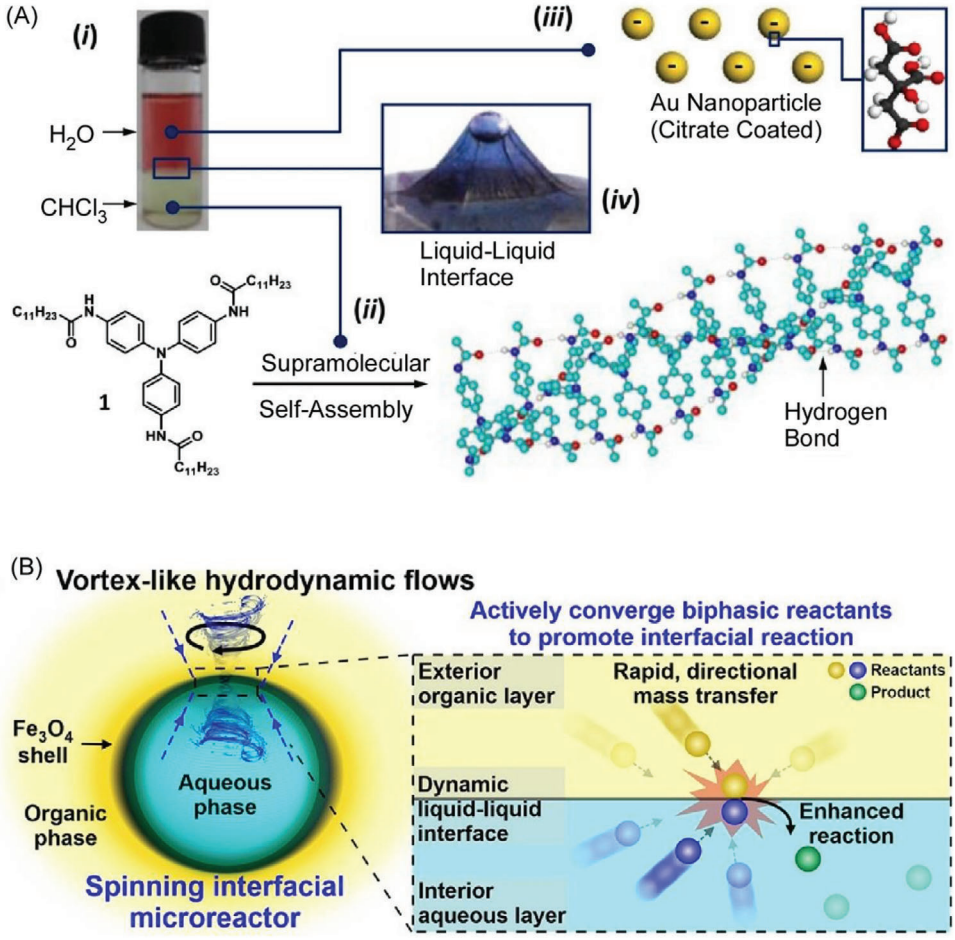


**Figure 4.** A) Supramolecular polymerization of triarylamine molecules at the chloroform–water interface where triarylamines in chloroform undergo supramolecular polymerization upon partial photooxidation and are organized into helical fibrils. Reproduced under terms of the CC-BY license.[81] Copyright 2017, American Chemical Society. B) Methodology for efficient interfacial reactions via magnetic effects using dynamic rotational motion to generate a vortex-like hydrodynamic flow and to allow reactants effectively accumulate at the immiscible liquid boundary. Reproduced with permission.[82] Copyright 2022, American Chemical Society.

nanoparticles, but also for applied research in materials science of anisotropic functional structures. Generalization of this methodology should also open the way for the development of anisotropic materials that can be freely combined with other organic molecules, covalent polymer ionomers, and other metal nanoparticles that can self-assemble in one dimension, including ionic groups.

Lee and coworkers presented a methodology for efficient interfacial reactions via magnetic effects (Figure 4B).[82] In this attempt, they created a magnetically responsive microscale liquid–liquid interface and used its dynamic rotational motion to generate a vortex-like hydrodynamic flow. This flow allowed reactants in different liquid phases to rapidly converge at the reaction point, and the interfacial reaction proceeded efficiently. In this liquid–liquid interface microreactor, reactants effectively accumulate at the immiscible liquid boundary by dynamic rotation and accelerate reactions at the interface. In other words, the dynamic manipulation of the liquid–liquid interface can be converted to the facilitation of chemical transformations. In one case, rotation of the liquid–liquid interface at 800 rpm increased the reaction efficiency by more than 500-fold and the apparent equilibrium constant by more than $10^5$-fold compared to a normal solution or no motion. This dynamic interfacial technique is versatile and also provides a methodology for effectively manipulating interfacial reactions beyond the thermodynamic limits of static conditions. The accelerated reaction avoids the external energy input and high concentration of reactants used in the past examples, making it an environmentally friendly chemical reaction and chemical nanoarchitectonics method. In addition to chemical synthesis, this method can be applied in the fields of environmental improvement and molecular recycling. As a method to promote multiphase reactions, it would be a method to support beneficial reactions in chemical, bio, energy, and environmental applications.

Regular structures such as metal-organic frameworks (MOFs)[83–85] and covalent organic frameworks (COFs)[86–88] have attracted attention in many fields. Liquid–liquid interfaces are used as a venue for nanoarchitectonics of these structures in two dimensions. For example, Li and co-workers reported the synthesis of a membrane with a two-dimensional, conjugated

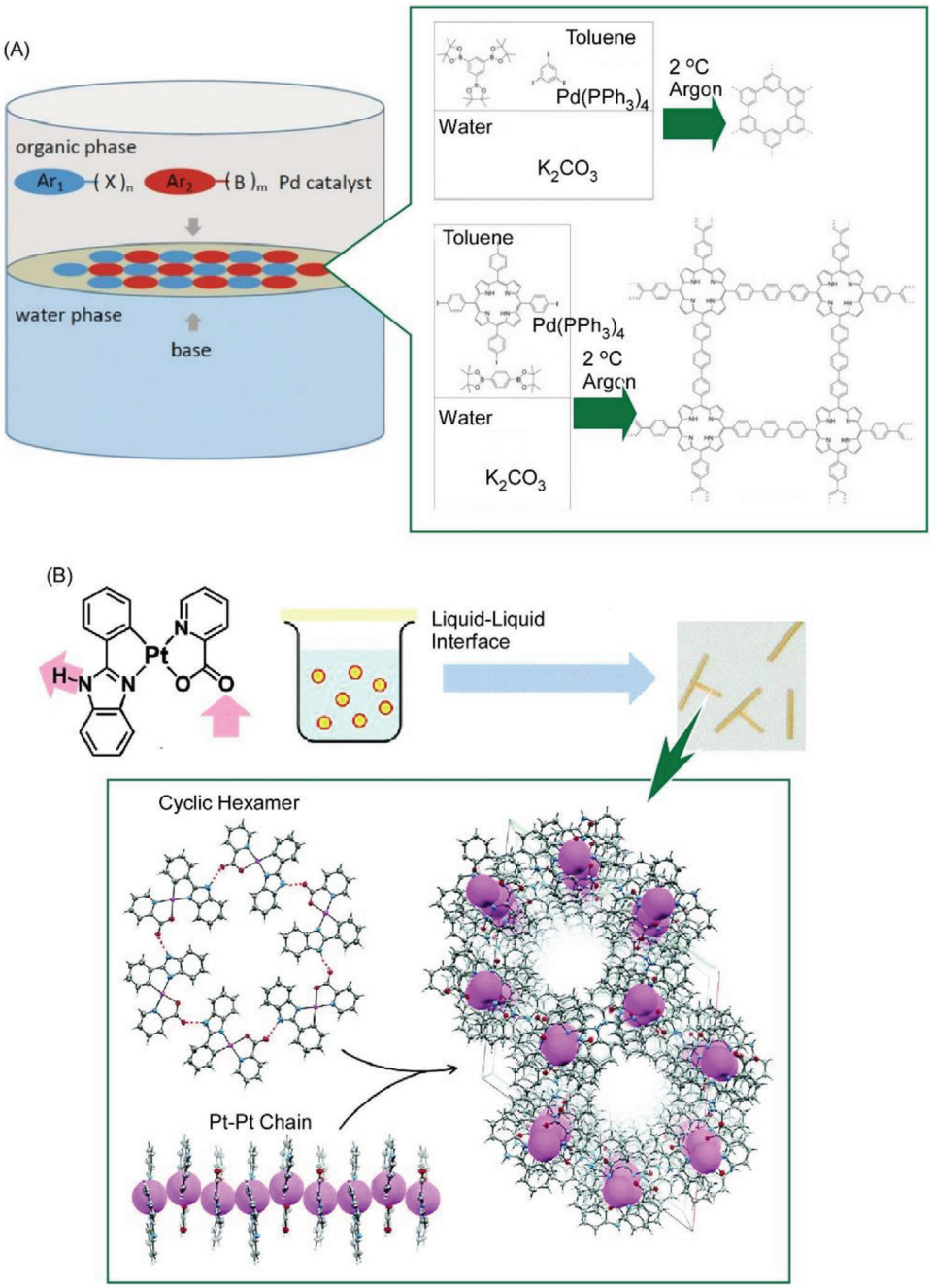


**Figure 5.** A) Synthesis of a membrane with a two-dimensional, conjugated organic framework linked by C–C bonds, in which Suzuki polymerization is carried out at the interface of water and toluene in a low-temperature environment in refrigerator. Reproduced with permission.[89] Copyright 2019, Wiley-VCH. B) Formation of a platinum(II) complex at the liquid–liquid interface with the pores nanoarchitectures. Reproduced with permission.[91] Copyright 2020, Royal Society of Chemistry.

organic framework linked by C–C bonds (**Figure 5**A).[89] This two-dimensional COF membrane preparation is a very simple and mild synthetic method, in which Suzuki polymerization is carried out at the interface of water and toluene in a low-temperature environment in refrigerator. Two types of COF membranes, porous graphene and porphyrin-containing two-dimensional COF, were demonstrated by this synthetic method. The synthesized porous graphene exhibited much higher carrier mobility than conventional two-dimensional COF membranes via −C=N− bonds. Thus these porous graphene-based two-dimensional COF films have potential applications in electronic devices and water splitting. In fact, it shows excellent catalytic activity for hydrogen evolution reactions comparable to nitrogen- and phosphorus-doped graphene. This two-dimensional nanoarchitectonics method could be extended to other similar reactions such as the Sonogashira and Heck reactions.

Two-dimensional COF membranes with an array of precisely controlled pore structures have great potential for applications such as permeable membranes with molecular discrimination capabilities. Han, Chung, and co-workers prepared flexible, self-supporting two-dimensional COF membranes at the liquid–liquid interface (the interface between water and dichloromethane) at room temperature and atmospheric pressure.[90] The COF membranes were nanoarchitectonized by adding tris(4-aminophenyl)amin and a catalyst to the aqueous phase and 2,4,6-triformylphloroglucinol to the dichloromethane phase at the interface. Two-dimensional COF thin films consisting of a highly ordered honeycomb lattice with controlled aperture size and channels were obtained. High solvent permeability was obtained due to the thin film structure. The solvent selectivity was the highest for acetonitrile among the tested solvents, followed by acetone, methanol, ethanol, and isopropanol. The pores also exhibited high nonpolar solvent permeability, depending on the polarity of the pores. The nanoarchitectonized two-dimensional COF membranes are expected to make a significant contribution to separation science and technology due to their high solvent permeability, precise molecular sieving effect, excellent shape selectivity, and sufficient flexibility.

Porous molecular crystals are expected to be a new generation of functional porous materials. Functional molecular crystals can be constructed at the liquid–liquid interface. Yoshida, Kato, and co-workers have demonstrated formation of a platinum(II) complex (cyclometalated Pt(II) complex [Pt(pbim)(pic)] (pbim = 2-phenylbenzimidazolate, pic = $\alpha$-picolinate) at the liquid–liquid interface (Figure 5B).[91] The obtained platinum(II) complex crystals were not obtained by common crystallization methods. In the crystallization process, Ostwald ripening is considered to have occurred in solution after the formation of seed crystals incorporating alkanes at the liquid–liquid interface. The stable formation of the crystals is thought to be due to the stabilization of the pores of the seed crystals by the inclusion of alkanes at the liquid–liquid interface. In addition, it may be possible to develop stimuli-responsive materials by guest exchange within the vacancies. The combination of immiscible solvents at the liquid–liquid interface is an attractive medium for crystallization nanoarchitecture and provides an efficient strategy for obtaining a variety of molecular crystals.

As some examples are given above, the liquid–liquid interface is a nanoarchitectonics field specifically for organic materials. It has been illustrated that supramolecular aggregates, supramolecular polymers, thin films of conducting polymers, polymer single-crystal-like capsules, assembled structures of various forms of block copolymers, two-dimensional COF films, complex crystals, and other specialty forms of materials can be obtained. The process can be governed not only by thermodynamic equilibrium but also by kinetic processes. This can be used to control the nanoarchitectonic structure in a transformable manner. Supramolecular aggregates and crystals with morphologies that cannot be obtained in bulk or solution systems can be obtained with exhibiting unique properties accordingly. In addition, the liquid–liquid interface becomes a site for promoting chemical reactions. Thus, the liquid–liquid interface provides nanoarchitectonics of organic materials with diverse properties in a manner different from that of three-dimensional systems, leading to diversification of functional manifestations.

## 3. Liquid–Liquid Interfacial Nanoarchitectonics, Inorganic

Nanoarchitectonics at the liquid–liquid interface can also be applied to inorganic and related materials. Gazil et al. reported a nanoarchitectonics method to synthesize metal nanoparticles for continuous shells by reaction at the liquid–liquid interface of emulsions (**Figure 6**A).[92] Using an Ouze system consisting of water, tetrahydrofuran, and butylhydroxytoluene, submicron-sized droplets (about 100 nm) with a narrow size distribution enriched in butylhydroxytoluene were prepared. When the reducing agent $NaBH_4$ is added to the aqueous phase and the metal precursors ($AuPPh_3Cl$, $Pd(PPh_3)_2Cl_2$) to the butylhydroxytoluene-rich droplets, nanoarchitectonics of various metallic objects are possible at the interface of the droplets. In other words, by in situ interfacial reduction of organometallic precursors in an emulsion system, metal shells consisting of ultrasmall Au nanoparticles, continuous Pd shells, and even bimetallic systems combining both were obtained in a single pot. The shell size of the nanoparticles was controlled by adding a water-soluble polymer during synthesis. This technique may be suitable for the preparation of size- and structure-controlled ultrasmall gold catalyst particles and therapeutic agents.

Nanoarchitectonics methods at the liquid–liquid interface are used to synthesize a variety of two-dimensional composite thin films. Menamparambath and co-workers reported one-pot synthesis of composite sheets of highly crystalline polypyrrole and $MnO_2$ at a liquid–liquid interface consisting of water and chloroform (Figure 6B).[93] Nanoparticle-attached oligomers/short chain polymers adsorb at the interface, forming microscale polypyrrole/$MnO_2$ sheets. Analysis by transmission electron microscopy (TEM) and atomic force microscopy (AFM) confirms that the morphology is that of an ultrathin sheet, within which highly crystalline $MnO_2$ nanoparticles of about 6 nm are uniformly distributed. This two-dimensional nanostructural tuning can be attributed to the high interfacial tension between water and chloroform, which facilitated the interfacial adsorption of polypyrrole oligomers with $MnO_2$ attached. This liquid interface nanoarchitectonics synthesis strategy is expected to lead to the development of functional polymer nanocomposite sheets and films, which can be applied to highly sensitive sensors.

As an investigation into the aggregation behavior of nanoparticles at the liquid–liquid interface, Shi and co-workers examined the attachment mechanism of nanoparticle surfactants generated by the interaction of nanoparticles and polymer ligands at the liquid–liquid interface.[94] **Figure 7** schematically illustrates the dissociation and degradation of nanoparticle surfactants at the oil–water interface by the introduction of competing ligands, inducing size-dependent non-jamming aggregation and suppressing jamming aggregation. Size-dependent assembly of nanoparticle surfactants at the interface can be induced or suppressed by tuning the binding energy of the nanoparticle surfactant to the interface and by controlling the packing state. Using the precisely designed size of nanoparticles and their characteristic fluorescence as a direct probe of their spatial distribution, the mechanism of nanoparticle surfactant attachment at the liquid–liquid interface was examined. Small nanoparticle surfactants that are loosely and irreversibly bound to the interface are displaced by larger nanoparticle surfactants. As a result, a size-dependent

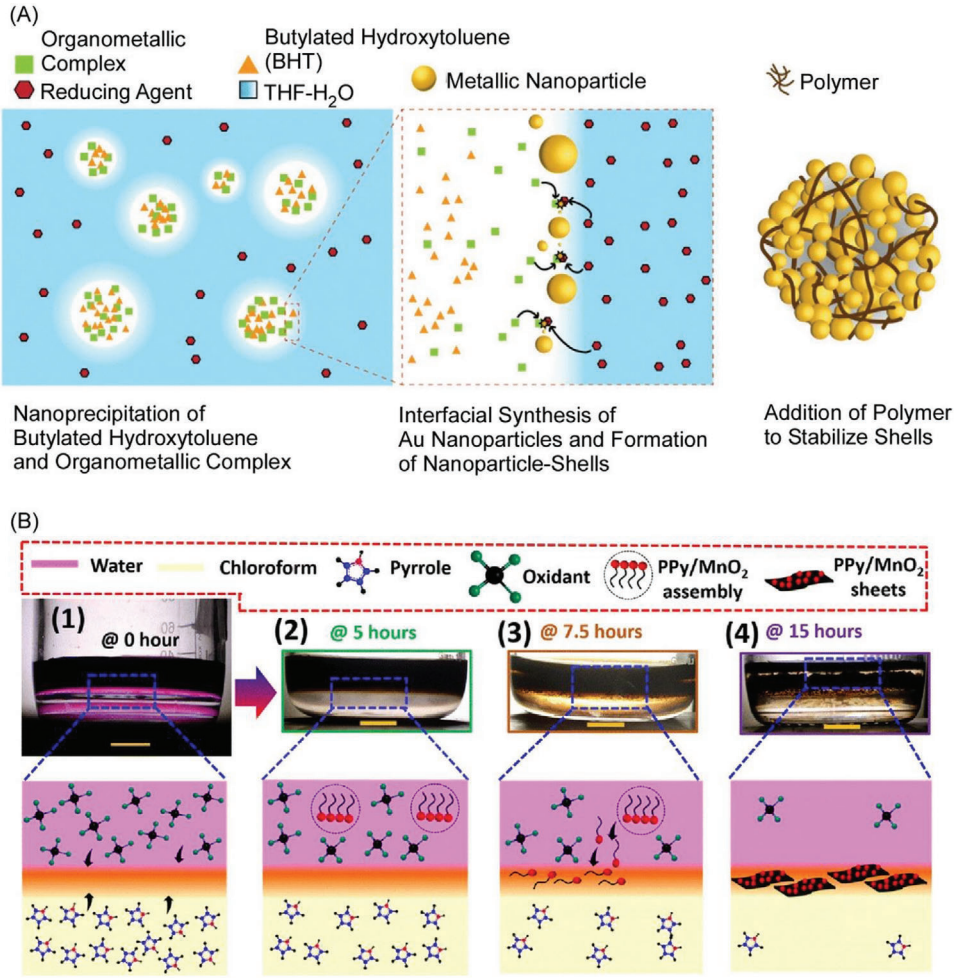


**Figure 6.** A) Nanoarchitectonics method to synthesize metal nanoparticle shells and continuous shells by reaction at the liquid–liquid interface of emulsions. Reproduced with permission.[92] Copyright 2022, Royal Society of Chemistry. B) One-pot synthesis of composite sheets of highly crystalline polypyrrole and $MnO_2$ at a liquid–liquid interface consisting of water and chloroform. Reproduced with permission.[93] Copyright 2022, Royal Society of Chemistry.

aggregation morphology of the nanoparticle surfactants at the interface appears. Conversely, if the smaller size nanoparticle surfactants are densely packed at the interface, size-dependent aggregation at the interface is completely suppressed. Such studies are important for understanding nanoparticle surfactant aggregation and jamming at the liquid–liquid interface. It paves the way for the creation of programmable liquid devices.

Inorganic crystals nanoarchitected at the liquid–liquid interface may exhibit better properties than bulk samples. Thin organic–inorganic $MAPbX_3$ perovskite single-crystal sheets are characterized by a low number of trapped states, high carrier mobility, long diffusion length, and large effective photosensitive area. However, $MAPbX_3$ single-crystals are very brittle and it is usually difficult to cut single-crystal sheets less than 100 µm in thickness. Liu and co-workers reported a method for synthesizing high-quality perovskite single crystals using a dimethicone/DMSO liquid–liquid interface (**Figure 8**A).[95] Using this liquid–liquid interface method, thin single-crystal $MAPbX_3$ sheets with thicknesses ranging from 1 to 50 µm were synthesized. The crystal quality of the obtained perovskite sheets was also improved. Compared to the conventional method, the DMSO biphasic system contributes to the interfacial diffusion of DMSO and produces single-crystal sheets with fewer defects on the top surface. By controlling the thickness of the liquid surface, vertical growth can also be limited and thickness can be controlled. Photodetectors made from this $MAPbX_3$ single-crystal sheet exhibit excellent response, external quantum efficiency, and ultrahigh sensitivity detection rates, with performance more than 500% higher than that of bulk crystal photodetectors. In addition, the sheet photodetectors maintained long-term stability for 4200 on/off cycles. The liquid–liquid two-phase interfacial nanoarchitectonics method is an ideal method for thin and high-quality single-crystal perovskite sheets, which is beneficial for device applications.

$Cs_2SnI_6$ perovskite has excellent air stability and high absorption coefficient, and is expected to have applications in photovoltaics and optoelectronics. Lian and co-workers have proposed a simple method for synthesizing $Cs_2SnI_6$ perovskite

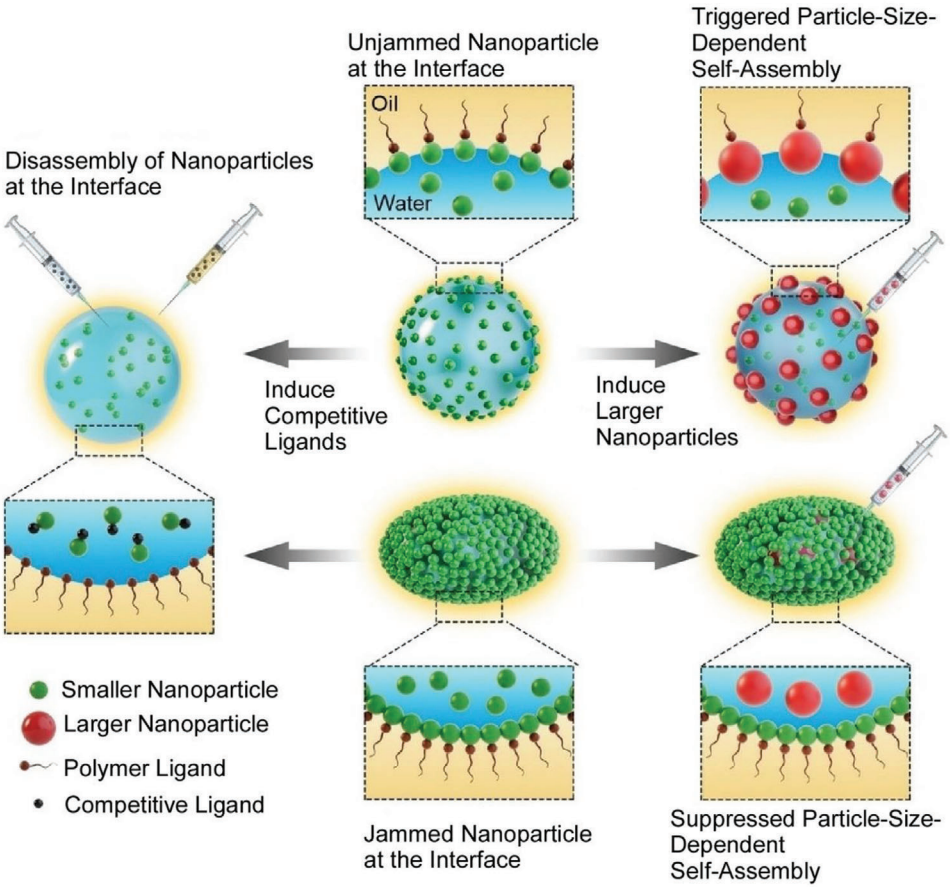


**Figure 7.** Dissociation and degradation of nanoparticle surfactants at the oil–water interface by the introduction of competing ligands, inducing size-dependent nonjamming aggregation and suppressing jamming aggregation. Reproduced with permission.[94] Copyright 2022, Wiley-VCH.

single crystals at the liquid–liquid interface (Figure 8B).[96] By controlling the degree of $Cs_2SnI_6$ supersaturation at the liquid–liquid interface, $Cs_2SnI_6$ crystals can be tuned between three-dimensional and two-dimensional growth. The growth mechanism and kinetics were analyzed by GIXD and in situ optical microscopy, respectively, and it was found that (111) stacking was observed in the out-of-plane direction in the initial stage, and that the transition to the three-dimensional growth region occurred with decreasing $SnI_4$ concentration. Advanced nonequilibrium growth allows controlled nanoarchitectonics of nanosheets with various shapes such as octahedrons, pyramids, hexagons, and triangles. For example, freestanding single-crystal two-dimensional nanosheets with a thickness of about 25 nm but a lateral size of sub-millimeter can be produced. Such two-dimensional nanosheets exhibit n-type conductivity with high carrier mobility. This liquid–liquid interfacial nanoarchitectonics method, which provides two-dimensional perovskite structures, is not only an example shown here, but is expected to become a method for synthesizing other non-layered compounds as two-dimensional structures.

Colloidosomes nanoarchitectonized at the liquid–liquid interface can be used as picoreactors. Ling and coworkers have developed a system that allows the isolation of solutions in picoliters and the monitoring of reactions in them (**Figure 9**).[97] Colloidosomes composed of silver octahedra were nanoarchitectonized at the interface of a decane–water emulsion. The particles act as two-phase picoreactors and can serve as a field for simultaneous in situ reaction monitoring of liquid–liquid interfacial reactions and molecular analysis during such reactions. In other words, plasmonic colloidosomes can separate ultratrace amounts of solution (<200 pL) and allow parallel surface-enhanced Raman scattering monitoring of multiple reactions simultaneously. In this picoreactor, the interfacial protonation of *p*-dimethylaminoazobenzene was monitored in situ using surface-enhanced Raman spectroscopy to identify the apparent rate constant for the first-order reaction. The study also revealed the presence of isomers with similar physical properties that are not distinguishable by other analytical methods. Ag octahedral to plasmonic colloidosomes can be combined with advanced analytical methods such as surface-enhanced Raman spectroscopy measurement techniques to analyze chemical reactions and nanoarchitectonic processes at the ultrafine level. This technology is expected to prove its worth in the fields of food chemistry, clinical analysis, and drug therapy.

Liquid–liquid interface nanoarchitectonics is said to be relatively flexible, which is also useful in the organization of rigid inorganic materials. Planar liquid interfaces are appropriate venues for the fabrication of nanosheet structures and two-dimensional

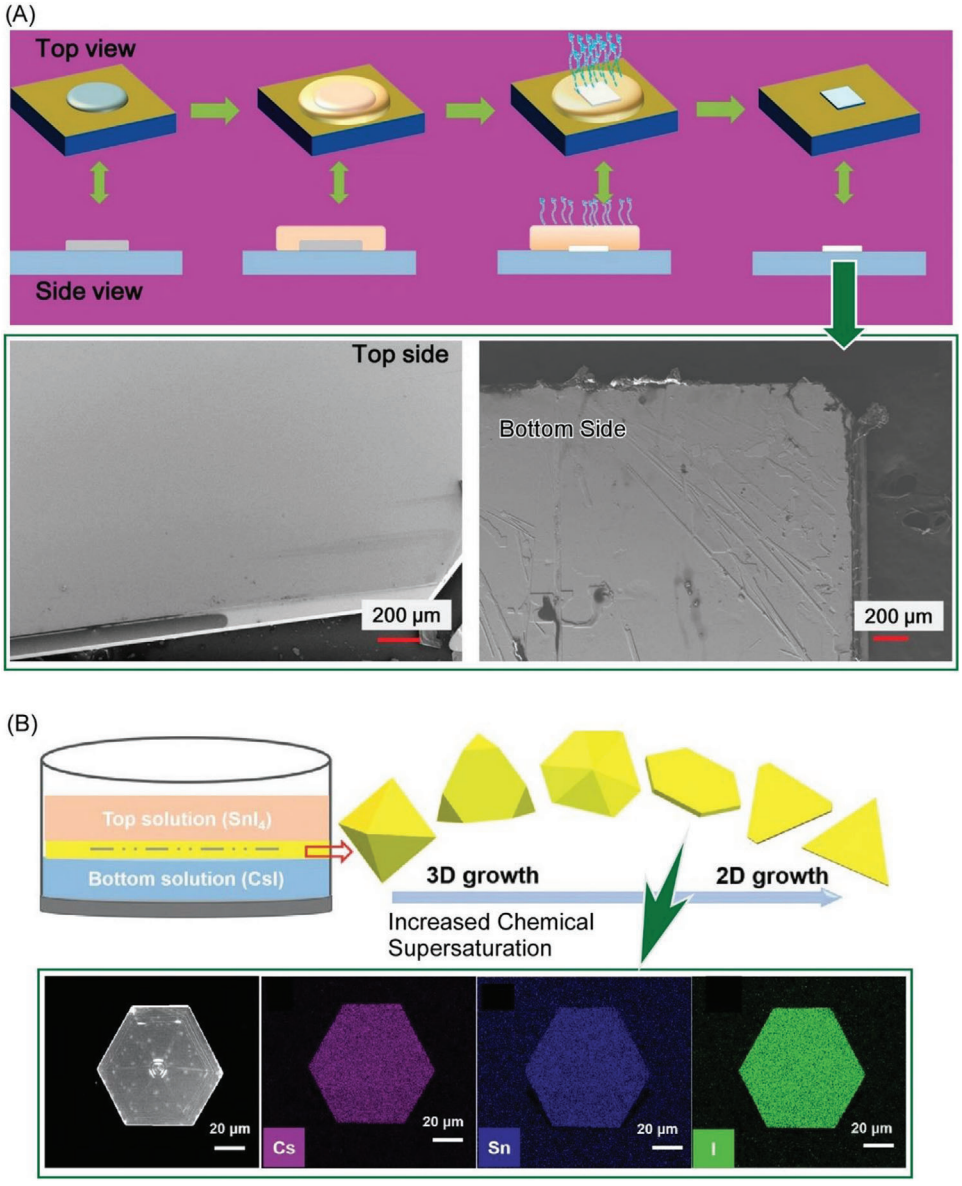


**Figure 8.** A) Method for synthesizing high-quality perovskite single crystals using a dimethicone/DMSO liquid–liquid interface where thin single-crystal $MAPbX_3$ sheets with thicknesses ranging from 1 to 50 μm were synthesized. Reproduced with permission.[95] Copyright 2021, American Chemical Society. B) Method for synthesizing $Cs_2SnI_6$ perovskite single crystals at the liquid–liquid interface, in which $Cs_2SnI_6$ crystals can be tuned between three-dimensional and two-dimensional growth. Reproduced with permission.[96] Copyright 2021, Wiley-VCH.

structures. Emulsions and droplet interfaces are also beneficial for the fabrication of closed spaces by colloidosomes, which gather inorganic unit units in three dimensions. Inorganic materials, which are considered to be stiff and difficult to deform, can be nanoarchitectonically transformed into various structures using the flexible field of the liquid–liquid interface.

## 4. Liquid–Liquid Interfacial Nanoarchitectonics, Carbon

A major category of functional materials is nanocarbons and the various carbon materials synthesized from them.[98–100] The liquid–liquid interface is also an important medium in carbon nanoarchitectonics. One promising method is the assembly and crystallization of fullerenes at the liquid–liquid interface.[101,102] The liquid–liquid interfacial precipitation method is a technique in which fullerenes such as $C_{60}$ and $C_{70}$ are dissolved in a good solvent to form a two-phase system with a poor solvent for fullerenes, and specific aggregates (crystals) are formed at the interface. One-dimensional,[103,104] two-dimensional,[105,106] three-dimensional,[107,108] and hierarchical fullerene assemblies[109,110] have been fabricated by this technique. Some recent examples of liquid–liquid interfacial nanoarchitectonics for the creation of carbon materials are introduced below.

Kim, Shrestha, and co-workers reported the preparation of short hollow rod-like fullerene assemblies (macaroni-fullerene

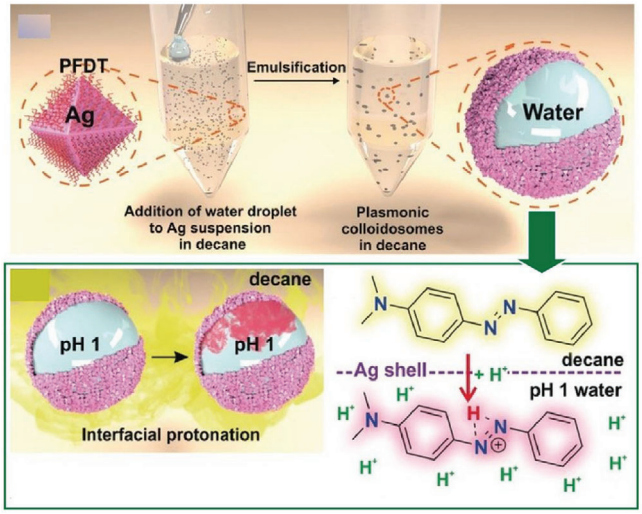


**Figure 9.** Isolation of solutions in picoliters and the monitoring of reactions in them using colloidosomes composed of silver octahedra nanoarchitectonized at the interface of a decane–water emulsion. Reproduced with permission.[97] Copyright 2016, Wiley-VCH.

crystals) at room temperature and their conversion into mesoporous carbon tubes for use as supercapacitors (**Figure 10**A).[111] First, self-assembled macaroni-fullerene crystals were prepared by dynamic liquid–liquid interfacial precipitation using *m*-xylene (good solvent) and isopropyl alcohol (poor solvent). The macaroni-fullerene $C_{60}$ crystals have a homogeneous morphology and narrow size distribution. The macaroni-fullerene crystals were further converted into mesoporous carbon with a high surface area by heat treatment at 900 °C in a nitrogen atmosphere. This carbonization process allowed the conversion to mesoporous carbon tubes with high surface area, high pore volume, and an interconnected mesopore structure, while maintaining the initial macaroni-like morphology in external appearance. This structure is a $\pi$-electron rich carbon source. In fact, the fabricated electrode exhibited high cycle stability, maintaining 96.8% of capacitance after 10 000 charge–discharge cycles. The new nanoporous carbon material obtained from the $C_{60}$ crystal could be an excellent electrode material for high-performance supercapacitors.

In other cases, structures created by liquid–liquid interfacial nanoarchitectonics were transformed by further solvent processes. For example, preparation of fullerene microtubes from a mixture of $C_{60}$ and $C_{70}$ by liquid–liquid interfacial precipitation and conversion of them into conical microhorns by exposure to a mixture of alcohol and mesitylene were demonstrated (Figure 10B).[112] In liquid interfacial precipitation using a $C_{60}/C_{70}$ mesitylene mixture and *tert*-butyl alcohol, $C_{70}$ molecules tend to form small aggregates in the initial stage due to the lower solubility of $C_{70}$ in the alcohol compared to $C_{60}$. These aggregates serve as cores for further growth of $C_{60}$ and $C_{70}$ co-crystals. In the fullerene microtubes, the concentration of $C_{70}$ is high in the center, while the tubular part at the end is mainly composed of $C_{60}$ with a smaller $C_{70}$ component. In other words, the concentration of $C_{70}$ should decrease as you move from the solid core in the center of the fullerene microtube to the hollow ends. Due to the balance between good and poor solvents, it is mainly in the $C_{70}$-rich region that the fullerenes are partially dissolved. When the fullerene microtubes are exposed to a mesitylene/*tert*-butyl alcohol mixture, the $C_{70}$-rich central partial core is preferentially dissolved in the solvent due to the high solubility of $C_{70}$ in mesitylene. As a result, one fullerene microtube separates into two fullerene microhorns. The resulting fullerene microhorn is charged, and silica particles are captured inside the horn due to the strong electrostatic interaction. Silica nanoparticles are preferentially trapped compared to fullerene $C_{70}$ particles, polystyrene latex particles, polystyrene hydroxide particles, and polystyrene carboxylate particles in the same size. The hollow structure of the microhorn can selectively tackle guest molecules and microscale objects and has potential applications in a variety of fields, including microencapsulation.

Various fullerene assemblies created by liquid–liquid nanoarchitectonics can also be converted into various hierarchical nanostructures by chemical etching using solvents through surface-selective chemical etching (Figure 10C).[113] First, fullerene $C_{60}$ nanorods, fullerene $C_{60}$ nanosheets, and fullerene $C_{70}$ cubes were synthesized by ultrasound-assisted liquid–liquid interfacial precipitation as a first step. Chemical etching of these crystals with ethylenediamine allows nanoarchitectonics of hierarchical structures according to the morphology of the assemblies. In the case of one-dimensional fullerene nanorods, they are selectively etched from the ends of the rods, yielding hollow-structured fullerene nanotubes. In the case of two-dimensional fullerene nanosheets, etching occurs mostly on the top and bottom surfaces of the sheet and only partially on the thin sides. In a three-dimensional fullerene cube, etching occurs on all sides of the cube. The result is a hierarchical structure with a gyroid-like morphology. These chemically etched fullerene nanostructures partially introduce amino groups to the surface. As a result, they exhibit excellent water dispersibility. They exhibit excellent vapor sensing performance selective for acid vapors such as formic acid and acetic acid, which is different from the high affinity for aromatic vapors such as benzene and toluene that normal fullerene aggregates exhibit. While lithographic techniques for nano- and microstructures usually involve expensive equipment, this simple and scalable solution process can be performed using only laboratory glassware. Because of these characteristics, it can be named "beaker lithography." It is a simple and scalable solution process, and it has potential applications in a wide range of fields, including biological research, drug carriers, ion sensing, separation, and energy storage.

The nanoarchitectonics of two-dimensional nanocarbons such as graphene at the liquid interface has also been investigated. Sakamoto, Nishihara, and coworkers reported bottom-up synthesis of all-carbon $\pi$-conjugated graphite nanosheets at the liquid–liquid interface (**Figure 11**A).[114] The specific method of liquid–liquid nanoarchitectonics involves placing a dichloromethane solution of hexaethylbenzene on a water layer containing a copper catalyst at room temperature and allowing the reaction to proceed at the liquid interface. The alkyne-alkyne homocoupling sequential reaction at the interface yields a multilayer graphdine with a thickness of 24 nm and a domain size of 25 μm or larger. Multilayer graphdine sheets have a 6 nm step at the edge. The same stacking as for multilayer graphadiynes was

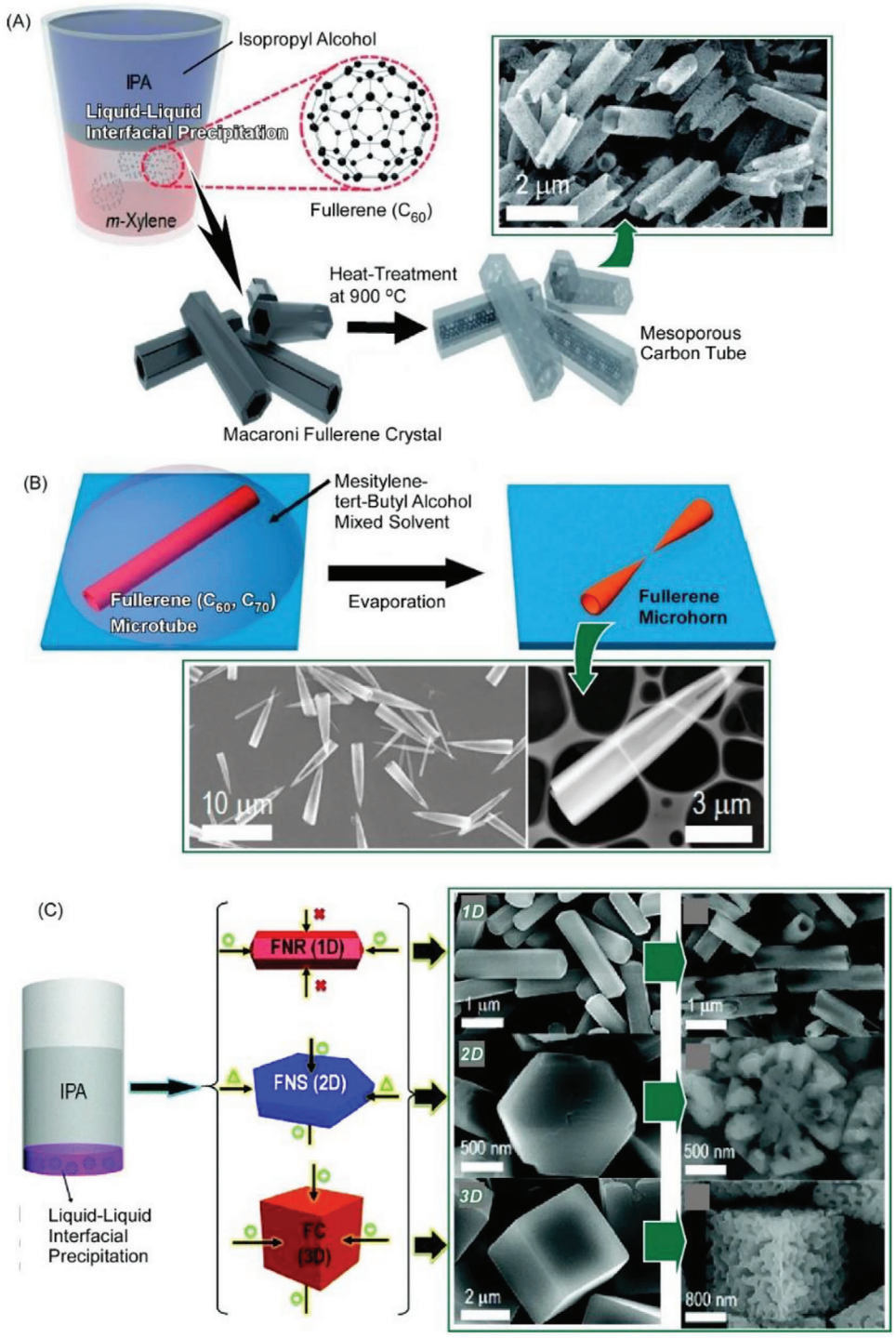


**Figure 10.** A) Preparation of short hollow rod-like fullerene assemblies (macaroni-fullerene crystals) at room temperature and their conversion into mesoporous carbon tubes for use as supercapacitors. Reproduced with permission.[111] Copyright 2021, Chemical Society of Japan. B) Preparation of fullerene microtubes from a mixture of $C_{60}$ and $C_{70}$ by liquid–liquid interfacial precipitation and conversion of them into conical microhorns by exposure to a mixture of alcohol and mesitylene. Reproduced with permission.[112] Copyright 2019, American Chemical Society. C) Fabrication of fullerene hierarchical structures by surface-selective chemical etching with ethylenediamine using fullerene nanorods, fullerene nanosheets, and fullerene cubes. Reproduced with permission.[113] Copyright 2020, Royal Society of Chemistry.

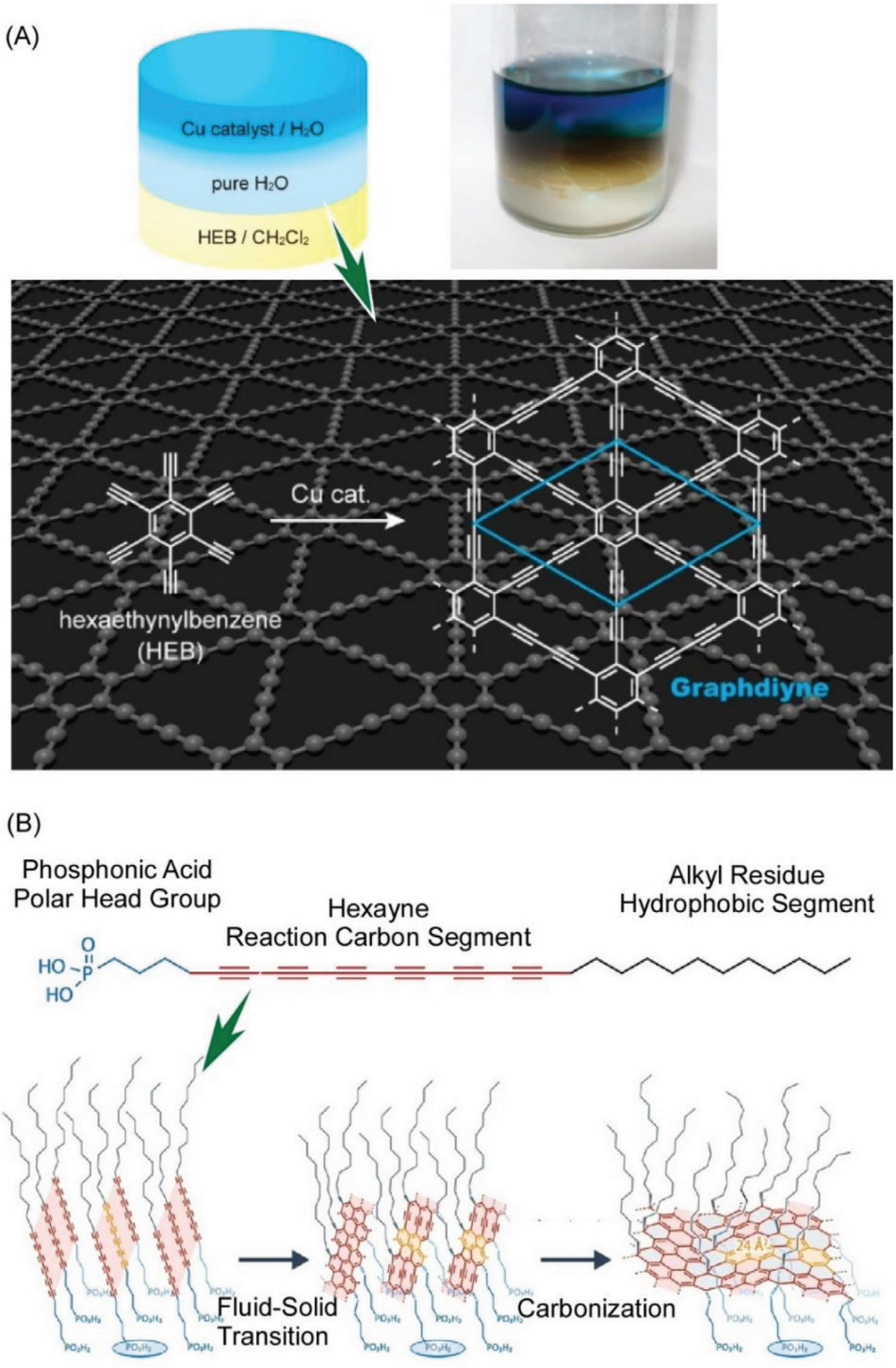


**Figure 11.** A) Bottom-up synthesis of all-carbon $\pi$-conjugated graphite nanosheets at the liquid–liquid interface upon placing a dichloromethane solution of hexaethylbenzene on a water layer containing a copper catalyst at room temperature and allowing the reaction to proceed at the liquid interface. Reproduced with permission.[114] Copyright 2017, American Chemical Society. B) Formation of a solid elastic film due to controlled two-dimensional polymerization of molecular surfactants at the interface and interfacial carbonization to finally generate a two-dimensional carbon nanoskin. Reproduced under terms of the CC-BY license.[115] Copyright 2022, Springer-Nature.

observed. Multifaceted microscopic analysis, including SEM, TEM, and AFM, revealed a well-defined hexagonal graphadiyne sheet with a narrow distribution of thickness. Well-defined regular hexagonal domains with a narrow distribution were found. The crystalline nature of the graphadiyne nanosheets was confirmed by two-dimensional GIWAXS. Due to the narrow domain size and thickness distribution, several-layer graphadiyne nanosheets with good crystallinity and low oxygen defect levels are nanoarchitectonically generated at the interface.

Frauenrath and co-workers used an oil–water interfacial environment to nanoarchitecture carbon nanoskins with both high stiffness and self-healing ability.[115] A solid elastic film is formed within a few seconds due to controlled diffusion of reactive molecular surfactants at the interface, as shown in Figure 11B. Subsequently, the surfactant by two-dimensional polymerization of 12 hexane carbon atoms occurs, and a final amorphous carbon monolayer composed of $C_{12}$ carbon tiles as a two-dimensional carbon nanoskin is finally generated through carbonization. This carbon nanoskin structure contains an amorphous, defect-rich monolayer of carbon decorated with dodecyl and phosphonatobutyl substituents. The overall thickness is a few nanometers, corresponding to the thickness of the first self-assembled surfactant monolayer. The carbon nanoskin exhibits an elastic modulus of over 40–100 GPa under bending deformation. This value is comparable to typical two-dimensional nanocarbon materials. The material is relatively brittle. However, nanoskins have the ability to self-repair and can be reshaped by mechanical stimuli. This property of being able to change its structure at will is unprecedented for carbon nanomaterials. Although the mechanism is different, it is reminiscent of biological membranes. Combined with microfabrication techniques such as 3D printing in liquids and microfluidic optics, it is expected that nanoarchitectonics materials with both mechanical strength and flexibility will be created.

Song et al. developed a novel nanocarbon material, "fullerphene" (**Figure 12**),[116] which uses a liquid–liquid interface to aggregate fullerene molecules in two dimensions and further carbonize them to form a two-dimensional nanocarbon nanoarchitectonics in a bottom-up manner. Its morphology and thickness are similar to graphene, a typical two-dimensional material. In this method, a two-dimensional graphene-like material, fullerphene, is created from a zero-dimensional fullerene. In the initial step of this process, the fullerene molecule is made amphiphilic by reacting in situ with ethylenediamine. The amphiphilic fullerene derivatives form a bilayer structure at the liquid–liquid interface of the emulsion. Upon heat treatment at 700 °C, nitrogen-doped ultrathin fullerphene films with hierarchical micro/mesoporous structures on the surface, are synthesized. The prepared fullerphene film has an ultrafine porous nanostructure consisting mainly of $sp^2$-bonded C atoms. It is doped with nitrogen atoms dominated by pyrrolic-nitrogen and quaternary-nitrogen. The latter feature allows the fullerphene films to selectively and repeatedly adsorb and desorb low molecular-weight carboxylic acid vapors through noncovalent interactions. Molecular-size micropores are derived during the conversion of the zero-dimensional unit matter fullerene into the two-dimensional fullerphene films. The formed pore structure is regarded as a molecular gate to discriminate size of guest molecules. The sensitivity of the quartz crystal microbalance (QCM) sensor modified with the fullerphene thin film depends not only on the acidity but also on the molecular size of the acid to be analyzed. The nanoarchitectonics approach to fullerphene thin films can be used to design functional nanomembranes with hierarchical porous structures consisting of micropores and mesopores on the surface, and to develop nitrogen-doped nanocarbon films.

The liquid–liquid interface is the site for nanoarchitectonics of various nanocarbons. A typical method is liquid–liquid interfacial precipitation, which exploits the difference in solubility of materials such as fullerenes between two different solvents. By combining this technique with postfabrication methods, it is easy to fabricate not only two-dimensional materials but also tubes, cube-shaped materials, and objects with hierarchical structures. Of course, the two-dimensionally confined space at the liquid–liquid interface is a powerful site for the creation of various two-dimensional materials. New materials such as all-carbon $\pi$-conjugated graphite nanosheets, carbon nanoskins, and fullerphene thin films are being created one after another.

## 5. Liquid–Liquid Interfacial Nanoarchitectonics, Bio

The liquid–liquid interface has been shown to be a powerful venue for nanoarchitectonics of organic materials, inorganic stuffs and nanocarbons. It can be extended to biomaterials and living cells. As a final example, the behavior of cells at the liquid–liquid interface and the integration of biomaterials that affect it are discussed in this section.

In particular, it is well known that physical microenvironments and mechanical stresses at interfaces and surfaces strongly influence cell behaviors such as cell adhesion, proliferation, and differentiation. Such studies are usually performed at the solid–liquid interface using solid substrates and culture media. However, little is known about the biological effects of fluid substrates, where viscoelastic stress is essentially absent, on the behavior of cells at the liquid–liquid interface. Minami et al. proposed the use of perfluorocarbons, which are less toxic to cells. C2C12 myoblast culture was examined using the water–perfluorocarbon interface as the liquid–liquid interface in a fluid microenvironment (**Figure 13**).[117] Results of in vitro culture at the water–perfluorocarbon interface show that MyoD is expressed normally even when growth factors are reduced to induce muscle differentiation. However, expression of myogenin, a myogenic regulatory factor (MRF) family gene, is markedly reduced, proving that MyoD upregulates myogenin on elastic and viscoelastic solid surfaces, which significantly alters cell differentiation behavior at the liquid–liquid interface. Not only such biological aspects, but also cells cultured at the water–perfluorocarbon interface were successfully transferred to the substrate using the Langmuir–Blodgett (LB) method. This means that nanoarchitectonics can be performed using living cells as materials. This interfacial culture system and application of the LB method is expected to be applicable to a wide variety of cells while preserving their biological functions. The liquid–liquid interface with perfluorocarbons will be beneficial for research in the field of mechanobiology. The introduction of the LB method is also expected to contribute to the fields of tissue engineering and stem cell research.

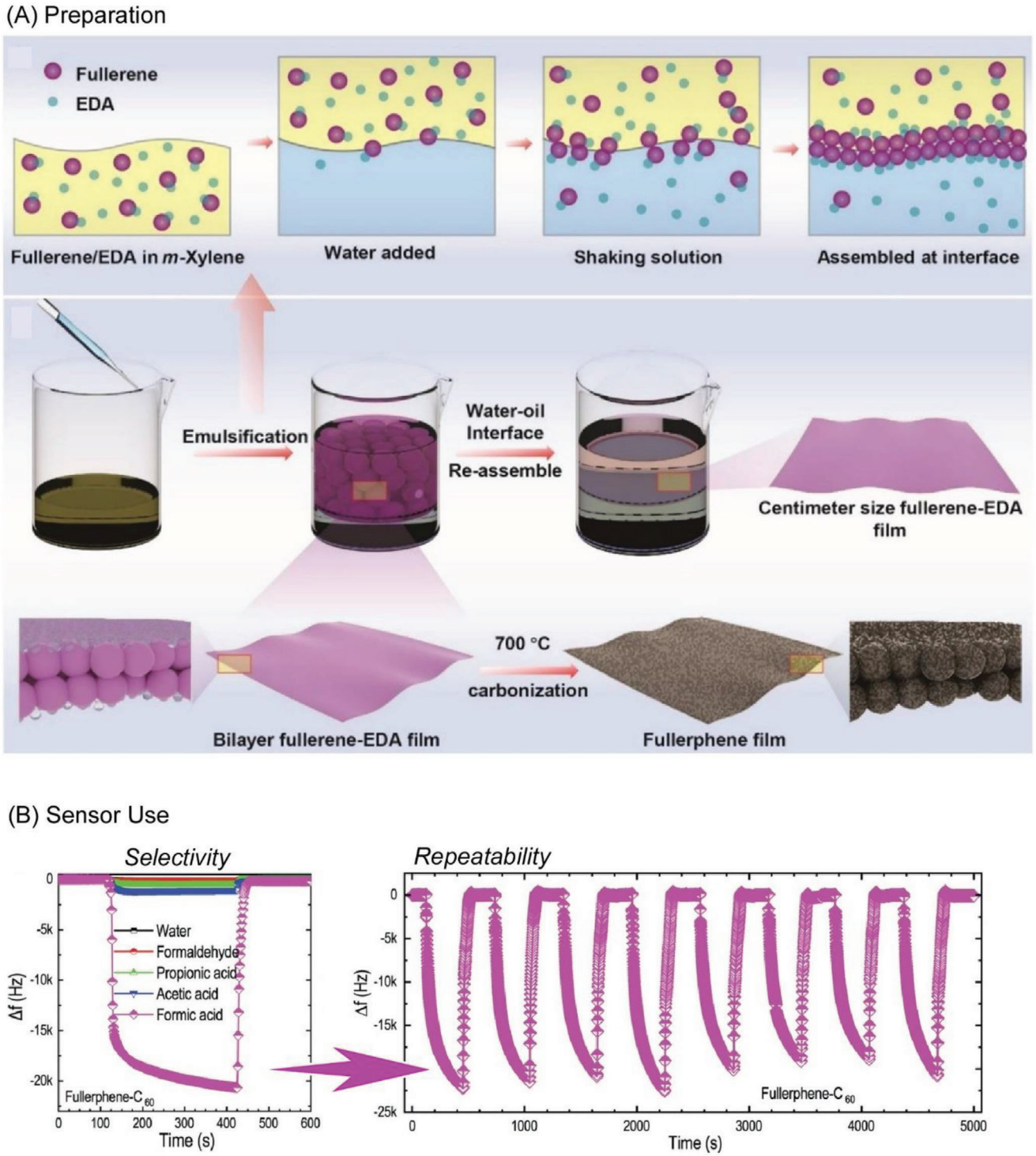


**Figure 12.** Novel nanocarbon material, fullerphene: A) preparation through liquid–liquid interfacial assembly of fullerene molecules and further carbonization to form a two-dimensional nanocarbon nanoarchitectonics. B) Responces of the quartz crystal microbalance (QCM) sensor modified with the fullerphene thin film with selective sensing of carboxylic acid guests. Reproduced with permission.[116] Copyright 2022, Wiley-VCH.

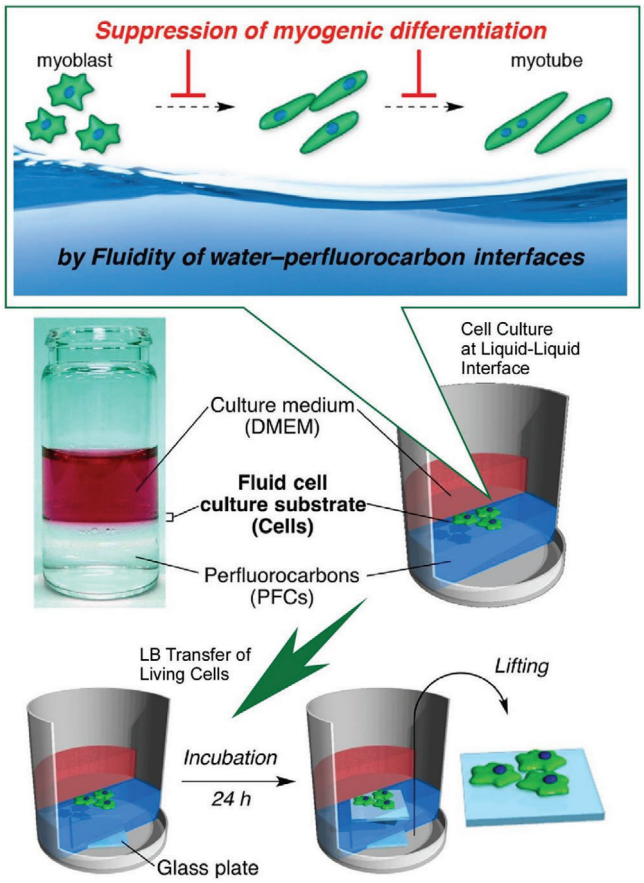


**Figure 13.** Culture of C2C12 myoblast culture using the water–perfluorocarbon interface as the liquid–liquid interface and Langmuir–Blodgett (LB) transfer of living cells. Reproduced with permission.[117] Copyright 2017, American Chemical Society.

As mentioned above, cell culture is possible on very low viscosity liquid interfaces such as fluorinated liquids and silicone oils. However, the relaxation rate at low viscosity liquid interfaces is too fast to allow stabilization of focal adhesions with lifetimes of minutes to hours. Such cell culture behavior is actually surprising. Gautrot and co-workers suggested that self-assembly of proteins to create mechanically strong enough nanosheets could aid cell spreading and growth on low-viscous liquid surfaces.[118] They propose that globular proteins such as albumin denature and react with other molecules to form nanosheet structures by hydrophobic cross-linking. Spontaneous protein nanosheet nanoarchitectonics at the liquid–liquid interface supports cell growth and culture at the liquid–liquid interface despite the lack of bulk mechanical properties of the culture substrate. In addition, Gautrot and co-workers extensively screened the effects of surfactants, proteins, oils, and cell types on cell culture at the liquid–liquid interface.[119] Interfacial microrheology combined with magnetic tweezers was used to correlate interfacial mechanical properties with stem cell proliferation. Multiscale viscoelasticity changes depending on the amorphous structure of two-dimensional nanosheets at the liquid–liquid interface and controls cell expansion. Protein amorphous nanosheets exhibit high elasticity despite low interfacial shear mechanical properties. This high elasticity makes them suitable for cell culture at the liquid–liquid interface. Adherent cells can grow while maintaining the cell phenotype. By successfully designing liquid–liquid interfacial systems in which interfacial shear and viscoelasticity can be skillfully controlled, it is also expected that cell behavior can be controlled in more detail.

Cellular functions such as cell proliferation and differentiation can be tuned by the mechanical cues that cells sense in the microenvironment. To understand such principles, Jia et al. examined in detail the behavior of human mesenchymal stem cells (hMSCs) at the liquid–liquid interface between perfluorocarbon solvent and culture medium (**Figure 14**A).[120] It was demonstrated that the self-assembled single-molecule protein nanosheets at the liquid–liquid interface are still rigid enough to support cell spreading without additional processing. In the reported case, fibronectin is incorporated into protein nanosheets. The high stiffness of the protein nanosheets causes cell spreading, growth of adhesions, and nuclear translocation of YES-related proteins. The mechanical response of cells to these protein nanosheets is mediated by a molecular clutch mechanism. Controlling protein packing at the liquid–liquid interface can fine-tune the dynamics of the protein layer and control cell behavior. Two perfluorocarbon phases, perfluorotributylamine and perfluorodecalin, are used. The packing of proteins in the two-dimensional nanoarchitecture of the nanosheets formed at the liquid interface between these two types and the culture aqueous solution was different. At the perfluorotributylamine interface, the protein molecules in the protein nanosheets were tightly packed. In this case, they were mechanically resistant enough to interact with cells, allowing focal adhesion growth and cell spreading. Conversely, when cells were cultured at the perfluorodecalin interface, the interactions between adjacent protein molecules were weak and fragile nanosheets were formed. In this case, the protein nanosheets quickly succumbed to the traction forces of the cells. As a result, cell spreading was hindered. In general, freestanding ultrathin protein nanosheets are very flexible and easily deformable. Cells perceive the protein nanosheets as softer. This understanding of cell culture at the liquid–liquid interface is expected to advance the nanoarchitectonics of next-generation stem cell culture materials and implant materials to contribute to regenerative therapies.

Jia et al. further identified the fact that protein nanosheets formed at the liquid–liquid interface interact with human mesenchymal stem cells to promote their neural differentiation (Figure 14B).[121] Protein nanosheets formed at the liquid–liquid interface act as adaptive structures that dynamically adapt to cell traction. In this process, the protein nanosheet is transformed into a hierarchical fibrous ultrastructure by the phenomenon of interfacial jamming. The elongated fibronectin fibers promote the formation of elongated focal adhesion structures. This change results in increased activation of focal adhesion kinases and promotes neural differentiation of stem cells. The detailed behavior is as follows. First, after 4 h of culture, clear ridges of protein nanosheets were observed at the cell periphery. This is considered to be the formation of the ridge due to the elastic force generated through the deformation of the protein nanosheets to counter the traction force by the cells. In response to this deformation, the protein aggregates are compressed and fine wrinkles appear as jams in the protein aggregates. The self-association

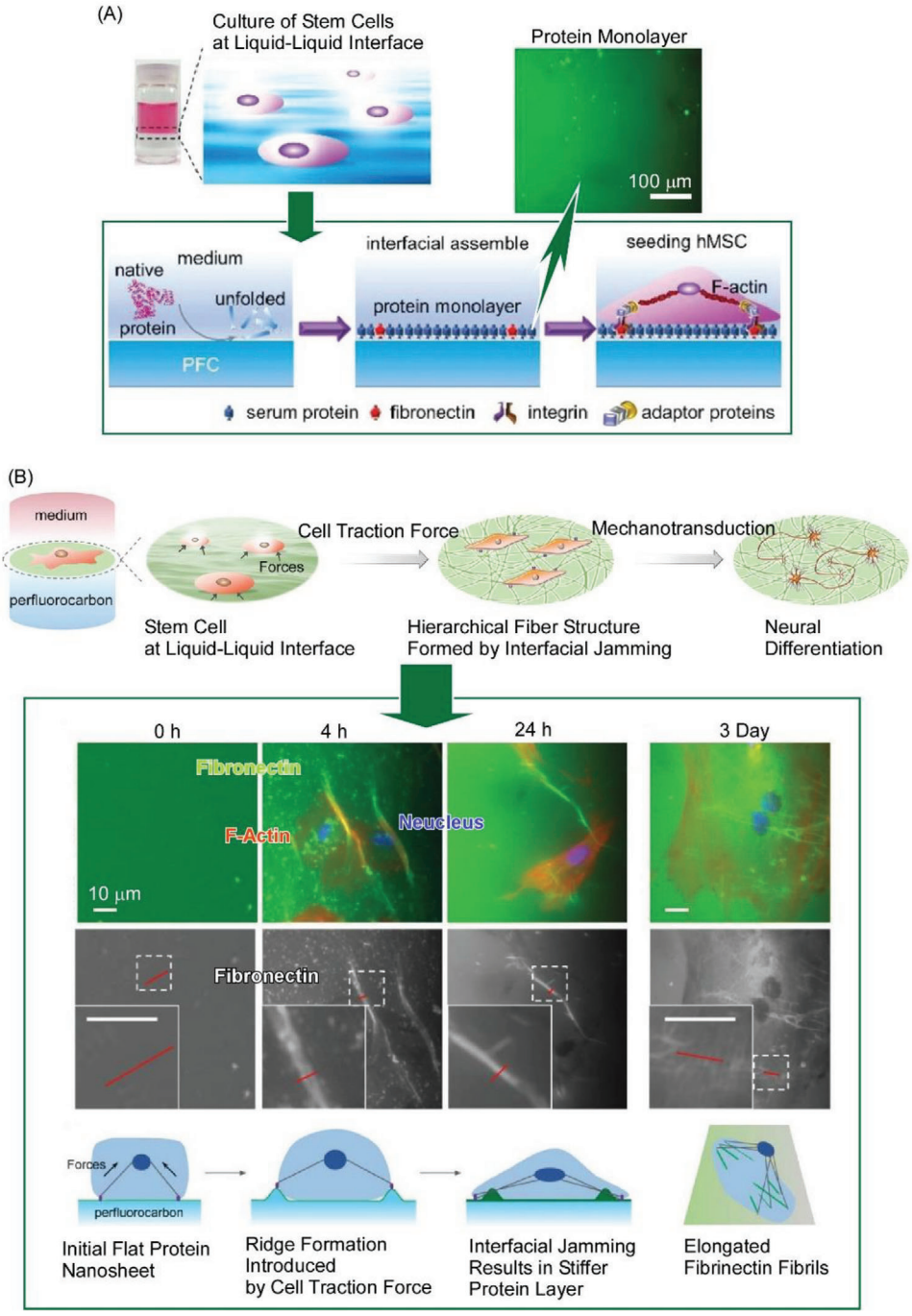


**Figure 14.** Behavior of human mesenchymal stem cells at the liquid–liquid interface between perfluorocarbon solvent and culture medium: A) supporting of cell spreading upon formation of single-molecule protein nanosheets. Reproduced with permission.[120] Copyright 2019, Wiley-VCH. B) Mutual interaction with protein nanosheets and human mesenchymal stem cells for promotion of their neural differentiation. Reproduced with permission.[121] Copyright 2020, Wiley-VCH.

sites of fibronectin are partially opened, promoting fiber formation. The deformation and jamming phenomena promote morphological changes to a solid fiber network and adaptively enhance mechanical properties, thus facilitating cell spreading. Over the next 3 days, fibronectin is further reorganized into a thin fiber structure along F-actin. This fiber structure is transmitted by human mesenchymal stem cells through the spatial arrangement of focal adhesions, resulting in optimal cytoskeletal tension and promoting neurogenesis. Cellular traction leads to spatial rearrangement of proteins in the extracellular matrix, induces membrane receptor clustering, activates signaling pathways, and ultimately leads to stem cell differentiation. A series

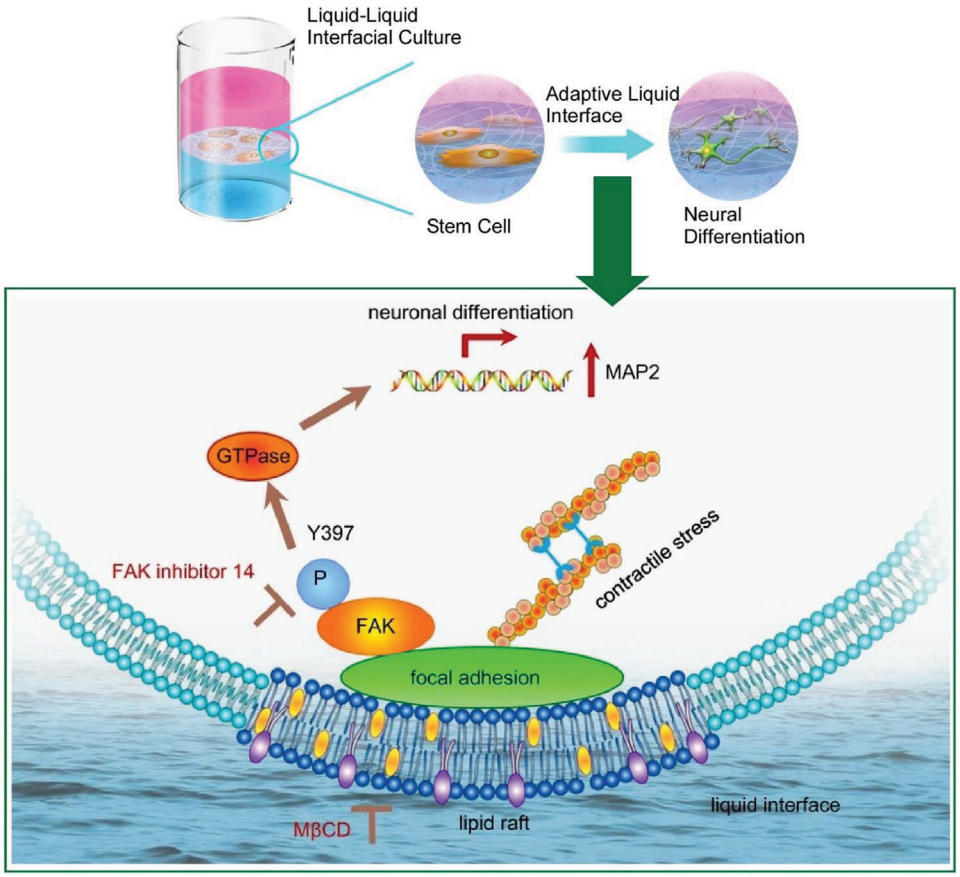


**Figure 15.** Two-dimensional network of protein nanofibrils at a liquid–liquid interface as an adaptive biomaterial for promotion of neuronal differentiation of human mesenchymal stem cells through a signaling mechanism involving focal adhesion kinase, where lipid raft microdomains in the plasma membrane were found to play a central role in the rapid adaptation of cells to the dynamic microenvironment at the liquid–liquid interface. Reproduced under terms of the CC-BY license.[123] Copyright 2022, Springer-Nature.

of results will help elucidate the feedback mechanisms that determine long-term stem cell fate and are useful for nanoarchitectonics of biomaterials at the appropriate liquid–liquid interface for tissue engineering and regenerative medicine.

Gautrot and co-workers demonstrated the culture of adherent stem cells, such as mesenchymal stem cells and primary keratinocytes, at the liquid interface.[122] The cell culture was to be mediated by the assembly of polymer nanosheets. The mechanical properties of the self-assembled nanosheets determine the proliferation and culture behavior of the stem cells. For example, keratinocytes spread on stiff poly(L-lysine) nanosheets established a structured actin cytoskeleton with stress fibers. In contrast, cells adhering to the soft poly(L-lysine)–oil interface showed actin-rich protrusions reminiscent of the early stages of cell proliferation. Jia et al. demonstrated that instead of flat protein nanosheets, a two-dimensional network of protein nanofibrils was used at a liquid–liquid interface as an adaptive biomaterial.[123] In this case, they promoted neuronal differentiation of human mesenchymal stem cells through a signaling mechanism involving focal adhesion kinase. In particular, lipid raft microdomains in the plasma membrane were found to play a central role in the rapid adaptation of cells to the dynamic microenvironment at the liquid–liquid interface (**Figure 15**). Cell adhesion molecules are internalized in the lipid rafts. This raft structure serves as an enrichment platform and facilitates the integration of large signaling complexes. These mechanisms allow cells to rapidly adapt to a constantly changing microenvironment. Lipid raft formation and focal adhesion kinase phosphorylation have been implicated in the differentiation of human mesenchymal stem cells at the liquid–liquid adaptive interface. Such nanoarchitectonics at the adaptive liquid–liquid interface is expected to lead to new developments in the control of stem cell differentiation. Other possible nanoarchitectonics include the incorporation of bioactive proteins and responsive polymers. This could be the basis for designing novel adaptive biomaterials for regenerative medicine and tissue engineering.

As mentioned above, the liquid–liquid interface is used for self-assembly of biomolecules and associated cell regulation. In particular, cell growth and differentiation take place at the liquid–liquid interface by using solvents with low biological impact, such as perfluorocarbons, as the organic solvent phase. At the liquid–liquid interface, proteins and other biomolecules self-assemble and spontaneously form nanostructures. The interaction with these structures regulates cell differentiation behavior. Research in this field has just begun and there are many unexplored areas. If various component structures are nanoarchitectonized at

the liquid–liquid interface and given functions such as stimulus responsiveness, more sophisticated cellular control will become possible. The day may come when nanoarchitectonics at the liquid–liquid interface can be said to control life.

## 6. Short Perspectives

As illustrated above, the liquid–liquid interface, whether organic, inorganic, nanocarbon, or biomaterials/cells, is an ideal site for nanoarchitectonics. The liquid–liquid interface can be varied in combination and size, and is dynamic and kinetic. The liquid–liquid interface is a place where the size, polarity, and environment can be freely designed while being versatile and dynamic. It is a place where substances that do not dissolve in the same solvent encounter. It is also a place where various components come together to form structures that can be transformed at will. Examples discussed in this paper alone including molecular aggregates, supramolecular polymers, thin films of conductive polymers, polymer single-crystal-like capsules, block copolymer assemblies, two-dimensional COF films, complex crystals, inorganic nanosheets, colloidosomes, fullerene assemblies and their hierarchical structures, all-carbon $\pi$-conjugated graphite nanosheets, carbon nanoskins, and fullerphene thin films have been used for nanoarchitectonics of various materials. Furthermore, at the liquid–liquid interface using perfluorocarbons and aqueous phases, cell differentiation can be controlled via the self-assembled structure of biomaterials. The nanoarchitectonics of the liquid–liquid interface can even be said to be a technology for manipulating life.

In addition to what has been described in this paper, the liquid–liquid interface has several other advantages. Although we have mainly used flat, macroscopic liquid–liquid interfaces, microscopic environments such as nanoemulsions and microemulsions can also be used for liquid–liquid interface nanoarchitectonics. In this case, countless liquid–liquid interfaces can be created in a small volume. This can be a great advantage for industrial applications of basic scientific findings. When size of emulsions are decreased, interfacial areas per volumes drastically increased. Therefore, developments of technology and science of nanoemulsions will promote usages of scientific knowledge of liquid–liquid nanoarchitectonics to industrial application as well as developments on scaling-up of entire solution systems.

As another advantage, there are an infinite number of combinations of liquid phases, and a variety of things can be incorporated as building blocks to nanoarchitectonically create functional structures. This situation is similar to the important role played by coacervates in the early stages of life. From viewpoint of long history of earth, liquid–liquid interface nanoarchitectonics in microspace has the potential to give birth to and evolve life. Nature has spent billions of years performing such natural nanoarchitectonics. We may be able to achieve advanced functional systems comparable to life through liquid–liquid interfacial nanoarchitectonics, using the scientific knowledge and technology we have developed. Perhaps, mankind may drastically accelerate these processes with machine learning[124,125] and materials informatics[126,127] based on artificial intelligence that we have recently developed. Nanotechnology, nanoarchitectonics, and materials informatics will architect materials from the nano to create the highest performing functional systems.[128] It is like the evolutionary process of life shortened by an overwhelming amount of time. The liquid–liquid interface will play an important role in this artificial evolutional process of functional materials developments.

## Acknowledgements

This study was partially supported by Japan Society for the Promotion of Science KAKENHI (Grant Numbers JP20H00392 and JP23H05459).

## Conflict of Interest

The authors declare no conflict of interest.

## Keywords

carbon, cells, films, interfaces, liquid, nanoarchitectonics, self-assembly

Received: July 5, 2023
Revised: July 28, 2023
Published online: August 28, 2023

[1] Y. Sugimoto, P. Pou, M. Abe, P. Jelinek, R. Pérez, S. Morita, Ó. Custance, *Nature* **2007**, *446*, 64.
[2] K. Harano, *Bull. Chem. Soc. Jpn.* **2021**, *94*, 463.
[3] R. Xie, Y. Hu, S.-L. Lee, *Small* **2023**, *19*, 2300413.
[4] K. Kimura, K. Miwa, H. Imada, M. Imai-Imada, S. Kawahara, J. Takeya, M. Kawai, M. Galperin, Y. Kim, *Nature* **2019**, *570*, 210.
[5] K. Tokunaga, F. Odate, D. Asami, K. Tahara, M. Sato, *Bull. Chem. Soc. Jpn.* **2021**, *94*, 397.
[6] J. Ghanam, V. K. Chetty, X. Zhu, X. Liu, M. Gelléri, L. Barthel, D. Reinhardt, C. Cremer, B. K. Thakur, *Small* **2023**, *19*, 2205030.
[7] D. Guo, R. Shibuya, C. Akiba, S. Saji, T. Kondo, J. Nakamura, *Science* **2016**, *351*, 361.
[8] G. Chen, F. Sciortino, K. Ariga, *Adv. Mater. Interfaces* **2021**, *8*, 2001395.
[9] K. Maeda, F. Takeiri, G. Kobayashi, S. Matsuishi, H. Ogino, S. Ida, T. Mori, Y. Uchimoto, S. Tanabe, T. Hasegawa, N. Imanaka, H. Kageyama, *Bull. Chem. Soc. Jpn.* **2022**, *95*, 26.
[10] K. Ariga, *Nanoscale Horiz.* **2021**, *6*, 364.
[11] R. P. Feynman, *Eng. Sci.* **1960**, *23*, 22.
[12] M. Roukes, *Sci. Am.* **2001**, *285*, 48.
[13] K. Ariga, K. Minami, M. Ebara, J. Nakanishi, *Polym. J.* **2016**, *48*, 371.
[14] K. Ariga, Q. Ji, W. Nakanishi, J. P. Hill, M. Aono, *Mater. Horiz.* **2015**, *2*, 406.
[15] K. Ariga, J. Li, J. Fei, Q. Ji, J. P. Hill, *Adv. Mater.* **2016**, *28*, 1251.
[16] L. Cao, Y. Huang, B. Parakhonskiy, A. G. Skirtach, *Nanoscale* **2022**, *14*, 15964.
[17] G. Chen, S. K. Singh, K. Takeyasu, J. P. Hill, J. Nakamura, K. Ariga, *Sci. Technol. Adv. Mater.* **2022**, *23*, 413.
[18] K. Ariga, M. Nishikawa, T. Mori, J. Takeya, L. K. Shrestha, J. P. Hill, *Sci. Technol. Adv. Mater.* **2019**, *20*, 51.
[19] S. Datta, Y. Kato, S. Higashiharaguchi, K. Aratsu, A. Isobe, T. Saito, D. D. Prabhu, Y. Kitamoto, M. J. Hollamby, A. J. Smith, R. Dalgliesh, N. Mahmoudi, L. Pesce, C. Perego, G. M. Pavan, S. Yagai, *Nature* **2020**, *583*, 400.
[20] K. Hamada, D. Shimoyama, T. Hirao, T. Haino, *Bull. Chem. Soc. Jpn.* **2022**, *95*, 621.
[21] Y. Domoto, M. Fujita, *Coord. Chem. Rev.* **2022**, *466*, 214605.

[22] J. Adachi, M. Naito, S. Sugiura, N. Ha-Thu Le, S. Nishimura, S. Huang, S. Suzuki, S. Kawamorita, N. Komiya, J. P. Hill, K. Ariga, T. Naota, T. Mori, *Bull. Chem. Soc. Jpn.* **2022**, *95*, 889.
[23] Y. Saito, C. Murata, M. Sugiuchi, Y. Shichibu, K. Konishi, *Coord. Chem. Rev.* **2022**, *470*, 214713.
[24] K. Ariga, *Small Sci.* **2021**, *1*, 2000032.
[25] L. Sutrisno, K. Ariga, *NPG Asia Mater.* **2023**, *15*, 21.
[26] R. B. Laughlin, D. Pines, *Proc. Natl. Acad. Sci. U. S. A.* **2000**, *97*, 28.
[27] K. Ariga, R. Fakhrullin, *Bull. Chem. Soc. Jpn.* **2022**, *95*, 774.
[28] K. Ariga, *Small Struct.* **2021**, *2*, 2100006.
[29] X. Shen, J. Song, C. Sevencan, D. T. Leong, K. Ariga, *Sci. Technol. Adv. Mater.* **2022**, *23*, 199.
[30] W. Hu, J. Shi, W. Lv, X. Jia, K. Ariga, *Sci. Technol. Adv. Mater.* **2022**, *23*, 393.
[31] K. Ariga, X. Jia, J. Song, J. P. Hill, D. T. Leong, Y. Jia, J. Li, *Angew. Chem., Int. Ed.* **2020**, *59*, 15424.
[32] K. Ariga, M. Shionoya, *Bull. Chem. Soc. Jpn.* **2021**, *94*, 839.
[33] M. Aono, K. Ariga, *Adv. Mater.* **2016**, *28*, 989.
[34] K. Ariga, *Mater. Chem. Front.* **2017**, *1*, 208.
[35] K. Ariga, Y. Yamauchi, *Chem. - Asian J.* **2020**, *15*, 718.
[36] X. Jia, J. Chen, W. Lv, H. Li, K. Ariga, *Cell. Rep. Phys. Sci.* **2023**, *4*, 101251.
[37] K. Ariga, L. K. Shrestha, *Adv. Intell. Syst.* **2020**, *2*, 1900157.
[38] S. J. Marrink, V. Corradi, P. C. T. Souza, H. I. Ingólfsson, D. P. Tieleman, M. S. P. Sansom, *Chem. Rev.* **2019**, *119*, 6184.
[39] S. Hirota, S. Nagao, *Bull. Chem. Soc. Jpn.* **2021**, *94*, 170.
[40] G. Kurisu, H. M. Zhang, J. L. Smith, W. A. Cramer, *Science* **2003**, *302*, 1009.
[41] M. Kosugi, M. Kawasaki, Y. Shibata, K. Hara, S. Takaichi, T. Moriya, N. Adachi, Y. Kamei, Y. Kashino, S. Kudoh, H. Koike, T. Senda, *Nat. Commun.* **2023**, *14*, 730.
[42] V. Cherezov, D. M. Rosenbaum, M. A. Hanson, S. G. F. Rasmussen, F. S. Thian, T. S. Kobilka, H. J. Choi, P. Kuhn, W. I. Weis, B. K. Kobilka, R. C. Stevens, *Science* **2007**, *318*, 1258.
[43] E. C. Greenwald, S. Mehta, J. Zhang, *Chem. Rev.* **2018**, *118*, 11707.
[44] Y. R. Kamimura, M. Kanai, *Bull. Chem. Soc. Jpn.* **2021**, *94*, 1045.
[45] S. Mehta, J. Zhang, *Nat. Rev. Cancer* **2022**, *22*, 239.
[46] K. Ariga, M. V. Lee, T. Mori, X.-Y. Yu, J. P. Hill, *Adv. Colloid Interface Sci.* **2010**, *154*, 20.
[47] K. Ariga, *Nanoscale* **2022**, *14*, 10610.
[48] K. Ariga, *Curr. Opin. Colloid Interface Sci.* **2023**, *63*, 101656.
[49] S. Clair, D. G. de Oteyza, *Chem. Rev.* **2019**, *119*, 4717.
[50] X. Xu, A. Kinikar, M. D. Giovannantonio, P. Ruffieux, K. Müllen, R. Fasel, A. Narita, *Bull. Chem. Soc. Jpn.* **2021**, *94*, 997.
[51] S. Kawai, O. Krejci, T. Nishiuchi, K. Sahara, T. Kodama, R. Pawlak, E. Meyer, T. Kubo, A. S. Foster, *Sci. Adv.* **2020**, *6*, eaay8913.
[52] S. Kawai, H. Sang, L. Kantorovich, K. Takahashi, K. Nozaki, S. Ito, *Angew. Chem., Int. Ed.* **2020**, *59*, 10842.
[53] K. Ariga, *Molecules* **2021**, *26*, 1621.
[54] M. Eguchi, A. S. Nugraha, A. E. Rowan, J. Shapter, Y. Yamauchi, *Adv. Sci.* **2021**, *8*, 2100539.
[55] K. Ariga, *Beilstein J. Nanotechnol.* **2023**, *14*, 434.
[56] K. Ariga, *Trends Chem.* **2020**, *9*, 779.
[57] K. Ariga, *ChemNanoMat* **2023**, 202300120.
[58] G. Rydzek, Q. Ji, M. Li, P. Schaaf, J. P. Hill, F. Boulmedais, K. Ariga, *Nano Today* **2015**, *10*, 138.
[59] M. Akashi, T. Akagi, *Bull. Chem. Soc. Jpn.* **2021**, *94*, 1903.
[60] K. Ariga, Y. Lvov, G. Decher, *Phys. Chem. Chem. Phys.* **2022**, *24*, 4097.
[61] Q. Ji, M. Miyahara, J. P. Hill, S. Acharya, A. Vinu, S. B. Yoon, J.-S. Yu, K. Sakamoto, K. Ariga, *J. Am. Chem. Soc.* **2008**, *130*, 2376.
[62] Q. Ji, S. B. Yoon, J. P. Hill, A. Vinu, J.-S. Yu, K. Ariga, *J. Am. Chem. Soc.* **2009**, *131*, 4220.
[63] K. Ariga, *Langmuir* **2020**, *36*, 7158.
[64] A. Kubo, M. Era, T. Narita, Y. Oishi, *Bull. Chem. Soc. Jpn.* **2021**, *94*, 2695.
[65] O. N. Oliveira Jr, L. Caseli, K. Ariga, *Chem. Rev.* **2022**, *122*, 6459.
[66] K. Ariga, *Acc. Mater. Res.* **2022**, *3*, 404.
[67] K. Ariga, *Chem. Mater.* **2023**, *35*, 5233.
[68] M. Ito, Y. Yamashita, Y. Tsuneda, T. Mori, J. Takeya, S. Watanabe, K. Ariga, *ACS Appl. Mater. Interfaces* **2020**, *12*, 56522.
[69] M. Ito, Y. Yamashita, T. Mori, M, C., T, F., J. Takeya, S. Watanabe, K. Ariga, *Langmuir* **2022**, *38*, 5237.
[70] V. Krishnan, Y. Kasuya, Q. Ji, M. Sathish, L. K. Shrestha, S. Ishihara, K. Minami, H. Morita, T. Yamazaki, N. Hanagata, K. Miyazawa, S. Acharya, W. Nakanishi, J. P. Hill, K. Ariga, *ACS Appl. Mater. Interfaces* **2015**, *7*, 15667.
[71] T. Mori, H. Tanaka, A. Dalui, N. Mitoma, K. Suzuki, M. Matsumoto, N. Aggarwal, A. Patnaik, S. Acharya, L. K. Shrestha, H. Sakamoto, K. Itami, K. Ariga, *Angew. Chem., Int. Ed.* **2018**, *57*, 9679.
[72] T. Maeda, T. Mori, M. Ikeshita, S. C. Ma, G. Muller, K. Ariga, T. Naota, *Small Methods* **2022**, *6*, 2200936.
[73] Y. Chevalier, M.-A. Bolzinger, *Colloids Surf., A* **2013**, *439*, 23.
[74] M. Kaneko, T. Nakayama, H. Seki, S. Yamamoto, T. Uemura, K. Inoue, S. Hadano, S. Watanabe, Y. Niko, *Bull. Chem. Soc. Jpn.* **2022**, *95*, 1760.
[75] Y. M. Ahmat, S. Kaliaguine, *Catal. Today* **2023**, *407*, 146.
[76] I. Robayo-Molina, A. F. Molina-Osorio, L. Guinane, S. A. M. Tofail, M. D. Scanlon, *J. Am. Chem. Soc.* **2021**, *143*, 9060.
[77] R. A. Lehane, A. Gamero-Quijano, S. Malijauskaite, A. Holzinger, M. Conroy, F. Laffir, A. Kumar, U. Bangert, K. McGourty, M. D. Scanlon, *J. Am. Chem. Soc.* **2022**, *144*, 4853.
[78] W. Wang, H. Qi, T. Zhou, S. Mei, L. Han, T. Higuchi, H. Jinnai, C. Y. Li, *Nat. Commun.* **2016**, *7*, 10599.
[79] K. Tiwari, P. Sarkar, S. Modak, H. Singh, S. K. Pramanik, S. Karan, A. Das, *Adv. Mater.* **2020**, *32*, 1905621.
[80] Y. Liu, X. Cui, Y.-I. Lee, H.-G. Liu, *Langmuir* **2022**, *38*, 4589.
[81] J. J. IV Armao, I. Nyrkova, G. Fuks, A. Osypenko, M. Maaloum, E. Moulin, R. Arenal, O. Gavat, A. Semenov, N. Giuseppone, *J. Am. Chem. Soc.* **2017**, *139*, 2345.
[82] L. S. Ng, C. Chong, X. Y. Lok, V. Pereira, Z. Z. Ang, X. Han, H. Li, H. K. Lee, *ACS Appl. Mater. Interfaces* **2022**, *14*, 45005.
[83] H.-C. Zhou, S. Kitagawa, *Chem. Soc. Rev.* **2014**, *43*, 5415.
[84] N. Hosono, *Bull. Chem. Soc. Jpn.* **2021**, *94*, 60.
[85] Y. Shan, G. Zhang, W. Yin, H. Pang, Q. Xu, *Bull. Chem. Soc. Jpn.* **2022**, *95*, 230.
[86] K. Geng, T. He, R. Liu, S. Dalapati, K. T. Tan, Z. Li, S. Tao, Y. Gong, Q. Jiang, D. Jiang, *Chem. Rev.* **2020**, *120*, 8814.
[87] D. Jiang, *Bull. Chem. Soc. Jpn.* **2021**, *94*, 1215.
[88] Y. Charles-Blin, T. Kondo, Y. Wu, S. Bandow, K. Awaga, *Bull. Chem. Soc. Jpn.* **2022**, *95*, 972.
[89] D. Zhou, X. Tan, H. Wu, L. Tian, M. Li, *Angew. Chem., Int. Ed.* **2019**, *58*, 1376.
[90] J. Liu, G. Han, D. Zhao, K. Lu, J. Gao, T.-S. Chung, *Sci. Adv.* **2020**, *6*, eabb1110.
[91] M. Kimura, M. Yoshida, S. Fujii, A. Miura, K. Ueno, Y. Shigeta, A. Kobayashi, M. Kato, *Chem. Commun.* **2020**, *56*, 12989.
[92] O. Gazil, N. Virgilio, F. Gauffre, *Nanoscale* **2022**, *14*, 13514.
[93] S. K. Chondath, A. P. K. Sreekala, C. Farzeena, S. N. Varanakkottu, M. M. Menamparambath, *Nanoscale* **2022**, *14*, 11197.
[94] B. Wang, B. Yin, Z. Zhang, Y. Yin, Y. Yang, H. Wang, T. P. Russell, S. Shi, *Angew. Chem., Int. Ed.* **2022**, *61*, e202114936.
[95] W. Xu, X. Wei, D. Zheng, W. Huang, P. Li, Y. Chen, F. Meng, J. Liu, *J. Phys. Chem. Lett.* **2021**, *12*, 10052.
[96] W. Zhu, J. Shen, M. Li, K. Yang, W. Bu, Y.-Y. Sun, J. Shi, J. Lian, *Small* **2021**, *17*, 2006279.
[97] G. C. Phan-Quang, H. K. Lee, X. Y. Ling, *Angew. Chem., Int. Ed.* **2016**, *55*, 8304.

[98] S. Iijima, *Nature* **1991**, *354*, 56.
[99] G. Singh, J. M. Lee, G. Kothandam, T. Palanisami, A. H. Al-Muhtaseb, A. Karakoti, J. Yi, N. Bolan, A. Vinu, *Bull. Chem. Soc. Jpn.* **2021**, *94*, 1232.
[100] M. S. Islam, Y. Shudo, S. Hayami, *Bull. Chem. Soc. Jpn.* **2022**, *95*, 1.
[101] M. Sathish, K. Miyazawa, *J. Am. Chem. Soc.* **2007**, *129*, 13816.
[102] L. K. Shrestha, Q. Ji, T. Mori, K. Miyazawa, Y. Yamauchi, J. P. Hill, K. Ariga, *Chem. - Asian J.* **2013**, *8*, 1662.
[103] J. Minato, K. Miyazawa, *Carbon* **2005**, *43*, 2837.
[104] Y. Mitake, A. Gomita, R. Yamamoto, M. Watanabe, R. Suzuki, N. Aoki, M. Tanimura, T. Hirai, M. Tachibana, *Chem. Phys. Lett.* **2022**, *807*, 140094.
[105] G. Chen, B. N. Bhadra, L. Sutrisno, L. K. Shrestha, K. Ariga, *Int. J. Mol. Sci.* **2022**, *23*, 5454.
[106] G. Chen, L. K. Shrestha, K. Ariga, *Molecules* **2021**, *26*, 4636.
[107] C. Park, E. Yoon, M. Kawano, T. Joo, H. C. Choi, *Angew. Chem., Int. Ed.* **2010**, *49*, 9670.
[108] G. Chen, F. Sciortino, K. Takeyasu, J. Nakamura, J. P. Hill, L. K. Shrestha, K. Ariga, *Chem. - Asian J.* **2022**, *17*, e202200756.
[109] S. Maji, L. K. Shrestha, K. Ariga, *Nanomaterials* **2021**, *11*, 2146.
[110] J. P. Hill, R. G. Shrestha, J. Song, Q. Ji, K. Ariga, L. K. Shresth, *Bull. Chem. Soc. Jpn.* **2021**, *94*, 1347.
[111] S. Maji, R. G. Shrestha, J. Lee, S. A. Han, J. P. Hill, J. H. Kim, K. Ariga, L. K. Shrestha, *Bull. Chem. Soc. Jpn.* **2021**, *94*, 1502.
[112] Q. Tang, S. Maji, B. Jiang, J. Sun, W. Zhao, J. P. Hill, K. Ariga, H. Fuchs, Q. Ji, L. K. Shrestha, *ACS Nano* **2019**, *13*, 14005.
[113] C.-T. Hsieh, S.-h. Hsu, S. Maji, M. K. Chahal, J. Song, J. P. Hill, K. Ariga, L. K. Shrestha, *Mater. Horiz.* **2020**, *7*, 787.
[114] R. Matsuoka, R. Sakamoto, K. Hoshiko, S. Sasaki, H. Masunaga, K. Nagashio, H. Nishihara, *J. Am. Chem. Soc.* **2017**, *139*, 3145.
[115] E. Bomal, P. Grandgeorge, R. J. Yeo, N. Candau, P. M. Reis, H. Frauenrath, *Nat. Commun.* **2022**, *13*, 4950.
[116] J. Song, T. Murata, K.-C. Tsai, X. Jia, F. Sciortino, R. Ma, Y. Yamauchi, J. P. Hill, L. K. Shrestha, K. Ariga, *Adv. Mater. Interfaces* **2022**, *9*, 2102241.
[117] K. Minami, T. Mori, W. Nakanishi, N. Shigi, J. Nakanishi, J. P. Hill, M. Komiyama, K. Ariga, *ACS Appl. Mater. Interfaces* **2017**, *9*, 30553.
[118] D. Kong, W. Megone, K. D. Q. Nguyen, S. Di Cio, M. Ramstedt, J. E. Gautrot, *Nano Lett.* **2018**, *18*, 1946.
[119] D. Kong, L. Peng, M. Bosch-Fortea, A. Chrysanthou, C. V. J.-M. Alexis, C. Matellan, A. Zarbakhsh, G. Mastroianni, A. del Rio Hernandez, J. E. Gautrot, *Biomaterials* **2022**, *284*, 121494.
[120] X. Jia, K. Minami, K. Uto, A. C. Chang, J. P. Hill, T. Ueki, J. Nakanishi, K. Ariga, *Small* **2019**, *15*, 1804640.
[121] X. Jia, K. Minami, K. Uto, A. C. Chang, J. P. Hill, J. Nakanishi, K. Ariga, *Adv. Mater.* **2020**, *32*, 1905942.
[122] D. Kong, L. Peng, S. D. Cio, P. Novak, J. E. Gautrot, *ACS Nano* **2018**, *12*, 9206.
[123] X. Jia, J. Song, W. Lv, J. P. Hill, J. Nakanishi, K. Ariga, *Nat. Commun.* **2022**, *13*, 3110.
[124] S. Wu, Y. Kondo, M. Kakimoto, B. Yang, H. Yamada, I. Kuwajima, G. Lambard, K. Hongo, Y. Xu, J. Shiomi, C. Schick, J. Morikawa, R. Yoshida, *npj Comput. Mater.* **2019**, *5*, 66.
[125] M. P. Neto, A. C. Soares, O. N. Oliveira Jr., F. V. Paulovich, *Bull. Chem. Soc. Jpn.* **2021**, *94*, 1553.
[126] K. Takahashi, Y. Tanaka, *Dalton Trans.* **2016**, *45*, 10497.
[127] Y. Oaki, Y. Igarashi, *Bull. Chem. Soc. Jpn.* **2021**, *94*, 2410.
[128] W. Chaikittisilp, Y. Yamauchi, K. Ariga, *Adv. Mater.* **2022**, *34*, 2107212.

**Katsuhiko Ariga** received his Ph.D. degree from the Tokyo Institute of Technology in 1990. He joined the National Institute for Materials Science (NIMS) in 2004 and is currently a group leader of the Supermolecules Group and a principal investigator of the World Premier International (WPI) Research Center for Materials Nanoarchitectonics (MANA). He is also appointed as a professor at The University of Tokyo. His expertise is in supramolecular chemistry and material nanoarchitectonics.